



Published in final edited form as:

Chem Rev. 2013 April 10; 113(4): 2842–2862. doi:10.1021/cr300468w.

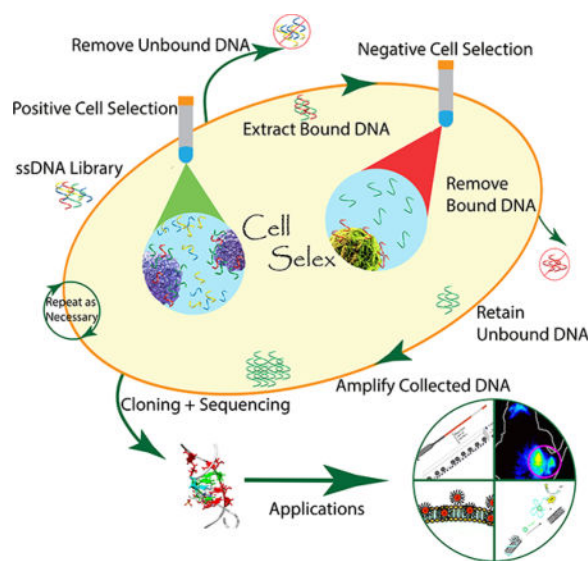
Aptamers from Cell-Based Selection for Bioanalytical Applications

Weihong Tan^{*,†,‡}, Michael J. Donovan^{†,‡}, and Jianhui Jiang^{*,†,‡}

[†]Molecular Science and Biomedicine Laboratory, State Key Laboratory of Chemo/Bio-Sensing and Chemometrics, College of Biology and College of Chemistry and Chemical Engineering, Collaborative Innovation Center for Chemistry and Molecular Medicine, Hunan University, Changsha 410082, People's Republic of China

[‡]Center For Research at Bio/nano Interface, Department of Chemistry and Department of Physiology and Functional Genomics, Shands Cancer Center, UF Genetics Institute and McKnight Brain Institute, University of Florida, Gainesville, Florida 32611, United States

Abstract



1. INTRODUCTION

Nucleic acids are the foundation of life. Specific sequences translate certain genetic traits, protein expression, and, ultimately, cellular function. Yet, nucleic acids not only store genetic information, but they can be very useful for the recognition of biological compounds. These molecules, when in single-stranded form, are called aptamers, which have gained much attention by harnessing the ability of nucleic acids to target certain biological molecules. More specifically, aptamers have the potential to be a very effective

^{*}Corresponding Author tan@chem.ufl.edu.

The authors declare no competing financial interest.

tool in bioanalysis. As the applications for aptamers evolve and the bioavailability of aptamers improves, the realization of their usefulness is increasing. Aptamers can be derived from a process termed “systematic evolution of ligands by exponential enrichment” (SELEX). To develop aptamers for cell membrane targets, a process termed cell-SELEX is used.

The development of aptamers for applications has greatly expanded since their inception approximately two decades ago. Many of these developments, particularly those for biomedical applications, are still at the research stage, but results are promising. One promising area is biomarker discovery. Much effort has been put into biomarker discovery, but improvement is still needed. Proteomic methods, such as two-dimensional gel electrophoresis (2D-GE) and differential imaging gel electrophoresis (DIGE), followed by mass spectrometry (MS) identification of proteins, have been employed for biomarker discovery, but with limited results. The elucidation of membrane proteins that are differentially expressed in disease is still a challenge.^{1,2} Furthermore, both MS and 2D-GE fail to give a full representation of cellular membrane proteins. MS serves as an effective tool for analytical purposes. However, its sensitivity is limited to the nanomolar range for protein concentrations, thus hindering its ability to detect a large portion of the proteome in plasma. For example, 2D-GE-MS only recognizes about 5% of an estimated 30% of total membrane proteins.³ Furthermore, stable isotope standards and capture by anti-peptide antibodies (SISCAPA) and multiple reaction monitoring (MRM) are limited to protein measurements under 100, meaning that a substantial amount of time and effort is needed to analyze a large number of proteins.⁴

This Review traces the development of aptamers and their use in biomarker discovery, detection, sensing, profiling, and characterizing of cells.

2. CELL-SELEX

Diagnostic techniques for cancer, such as computed tomography (CT), magnetic resonance imaging (MRI), and positron emission tomography with radiolabeled 2-fluoro-deoxy-glucose (FDG PET), have relied on the morphological changes of normal cells into tumors. However, these techniques only assess anatomical changes or nonspecific glucose metabolism.⁵ They cannot monitor molecular-level changes in normal cells. Accurately predicting the development of cancer depends on the detection and measurement of such nanoarchitectural changes, and this can now be done with the aid of aptamer probes for in vivo targeting of cells, in vivo imaging of proteins or small molecules, and a myriad of other biomedical applications.

2.1. Historical Context

The word aptamer derives from the Latin word *aptus*, which means to fit, and the Greek *meros*, meaning region.⁶ The first papers on aptamers were published in 1990 by Ellington and Gold.^{6,7} Nucleic acid aptamers are single strands of DNA or RNA with a length in the range of 10–100 nucleotides (nt), which are produced from a process termed “systematic evolution of ligands by exponential enrichment” (SELEX). The essence of an aptamer molecule is its three-dimensional structure arising from a folded single-stranded nucleic acid

(usually 20–60 bases). DNA and RNA are not limited in function to storing and transmitting genetic information; they also interact with other molecules, such as proteins. Aptamers have a very highly ordered tertiary structure, which allows them to form stable complexes with different targets, such as proteins.^{8–12} Their high binding affinity and specificity have garnered considerable scientific interest. SELEX was first used to generate these aptamers for known, targeted molecules. However, because cell-SELEX is intrinsically able to target membrane differences between cell lines, aptamers can now be selected for unique cellular molecules in their native state on live cells.

Aptamers can be referred to as “chemical antibodies”, but the term does not address the number of advantages that aptamers have over antibodies. Aptamers are economical, easy to synthesize and modify, possess long-term stability, exhibit low immunogenicity, and have greater tissue penetration than antibodies.^{13,14} Furthermore, aptamers can be developed in vitro, whereas antibodies need to be developed in vivo. The need to rely on a living organism for production can create anomalies among different batches and limit the ability to create antibodies for toxic targets.

SELEX can be performed for a variety of targets, from simple organic and inorganic molecules to peptides, proteins, and even live cells. The desired platform incorporated may change according to the intended application. Selection against proteins has been the traditional platform. By selecting against purified proteins, specific enrichment can be obtained if the target protein assumes a stable conformation. This method has allowed for high-affinity aptamers to be selected against many targets; examples of targets include, but not limited to, MUC1 peptides,¹⁵ extracellular domain of prostate-specific membrane antigen (PSMA),¹⁶ cell adhesion molecule P-selectin,¹⁷ and protein tyrosine phosphatase 1B (PTP1B).¹⁸ However, extracellular proteins within biology are much more complicated than purified proteins used for targeting. That is, proteins may be present in a modified state or can be masked in a physiological context. Under these circumstances, the aptamers might not recognize the natural structure of some proteins. Liu et al. selected RNA aptamers against the histidine-tagged EGFRvIII ectodomain produced by the *Escherichia coli* expression system.¹⁵ Although the generated aptamers exhibited high affinity and specificity for the in vitro purified protein, they did not bind to the full-length EGFRvIII protein expressed on the surface of eukaryotic cells, probably because a post-translational modification altered the structure of EGFRvIII. Therefore, to develop aptamers more suitable for biological applications, the process termed cell-SELEX was developed. Cell-SELEX targets whole, live cells, whereas SELEX targets isolated molecules. This ensures that the aptamers will target proteins in their native conformations. Although many of the examples throughout this Review will focus on cancer cells, Liu et al. demonstrate that SELEX may be used with a variety of cells. Additionally, Jaykus et al. have developed an aptamer for *Campylobacter jejuni*, species of bacteria that is associated with food illnesses.¹⁹

A cell's surface is complex and has many different molecules, especially proteins. Cell-SELEX can produce aptamers that specifically bind to a certain cell line based on these unique extracellular characteristics; thus, no prior knowledge of cell-surface marker proteins is required. Recently, SELEX has been performed against cancerous tissue. Li et al. have

performed SELEX against paraffin-embedded tissue samples from ductal carcinomas while using adjacent normal tissue for the negative selection.²⁰ The plasticity of aptamer selection was able to produce the aptamer BC15, which specifically recognizes breast cancer cells. The protein targeted by this aptamer was determined to be hnRNP A1.

Some drawbacks are, however, apparent. For instance, the DNA polyanion and the cell surface, which possesses a net negative charge, should repel one another; however, it is believed that the structure-related binding between the aptamer and the target will be able to overcome the repulsion force. The presence of divalent cations could also help to shield and reduce the effect of the DNA-negative charge. Also, the DNA backbone can nonspecifically interact with arginine or lysine and other side chain molecules that can potentially reduce the selectivity of generated aptamers. Still, these nonspecific interactions can be overcome through the evolutionary process of SELEX, as the specific binding of the 3D structure of the DNA sequences greatly outperforms the random nonspecific binding. As the evolutionary process proceeds, the nonspecific interactions are minimized to a point where they are negligible.

2.2. Design of Selection Process

PCR is a fundamental part of cell-SELEX. Therefore, it is imperative to use primers with high PCR amplification efficiency. Prior to the selection process, optimization of the annealing temperature and concentration of PCR reagents need to be performed. After the first round of PCR, three different PCR amplifications are performed for (i) amplification of the entire pool, (ii) optimization of the number of cycles for preparative PCR, and (iii) preparation of PCR for the next round of selection. For the subsequent rounds of selection, only (ii) and (iii) are performed.

Three main phases occur during cell-SELEX: incubation, partitioning, and amplification. Figure 1 illustrates the process. A library of up to 10^{16} DNA sequences is used to generate aptamers.²¹ The selection begins with the large pool of nucleic acids that is incubated with the target cell line. The large pool ensures the high diversity in forming different three-dimensional structures to fit into the binding pockets of various targets.^{21–23} The positive cell line has been removed from the cell culture media and washed. The cells incubated with the ssDNA are placed on a rotary shaker at a specific temperature. The unbound DNA is washed away, and bound sequences are eluted. This elevated temperature can allow for the DNA to be collected by disrupting the interaction between DNA and protein by the denaturing of the cell-surface proteins. Furthermore, DNA folding is distorted, allowing for the release of DNA from the target protein. Also, the DNAase that is potentially released from cell membrane disruption is inactivated at this temperature, weakening its ability to digest the DNA aptamer. The DNA that binds to the target cell line is collected and then incubated with the negative cell line. The DNA that remains after using a negative selection will be amplified (i.e., the DNA that does not bind to the negative cells). The antisense strand is retained, while the sense strand is eluted. This eluted ssDNA pool from the first round of selection is then used as the library for the next round of selection. It is important to note that an aptamer can still be produced for a certain protein that is present on both cell lines, as long as the presence of the protein is greater in the positive cell line than in the

negative cell line. A protein that is twice as abundant in the positive cell line can be improved by a factor of 2^9 after 10 rounds of selection, presuming certain conditions are met, such as maintaining the same cell concentration between positive and negative cell lines and ensuring high affinity of the aptamer.²⁴

By exponentially amplifying the collected DNA, an ample supply of unique sequences binding to the target cell line is guaranteed. Multiple rounds of selection are performed until families of aptamers are produced that have high binding affinity toward the target cell line. It is this multiplicity that limits the effect of stochastic cellular membrane differences among cell lines. Although aptamer affinity can be tested using flow cytometry, it is first necessary to separate the dsDNA created from the symmetrical PCR for the preparative PCR so that the FITC-labeled sequence can be recovered. To accomplish this, the sense strand of the primer is labeled (i.e., with a fluorophore), and the antisense strand is labeled at the 5'-end (i.e., with biotin). These sense strands are separated from antisense strands.

As the selection process progresses, flow cytometry may be used to monitor the progress. Potential aptamers that recognize any characteristics on the cell surface will show a fluorescence signal intensity that is significantly higher than that of the unselected control library (Figure 2). Screening should be repeated to confirm the results. Candidates that cannot bind at these concentrations should be discarded. Furthermore, if the control cells show a fluorescence signal, then negative selection is inefficient. To account for this, the number of control cells must increase along with an increase in incubation time.

The overall success of cell-SELEX can largely depend on the negative cell line because many cell receptors for a given cancer cell line are also possessed by normal cells. Because we do not want to target those receptors, the negative cell line is used to remove any DNA that binds to both the positive and the negative cell lines, leaving behind just the DNA sequences that bind to the unique extracellular membrane of the positive cells. The aptamer sequences that bind to the negative cell line are discarded, while the remaining sequences are kept for amplification in the next round of selection. Generally, around 20 rounds of cell-SELEX are required to achieve aptamers with the highest affinity toward the target cell line. However, aptamers with high affinity and specificity have been isolated after a much lower number of rounds. Table 1 shows certain combinations of cell lines that have previously been used to generate high-affinity and specific aptamers. For example, when developing an aptamer for a breast cancer cell line, a cell line that has a similar membrane composition is chosen to serve as the negative cell line. The closer the positive and negative cell line resemble each other, the more specific the aptamer will be.

Similar to aptamers selected against purified proteins, aptamers from cell-SELEX can also be analyzed to obtain the binding motif and be postengineered to enhance their affinity or functionality.^{28–30} For example, Sgc8c was cut from the Sgc8 sequence obtained from cell-SELEX. Further modification of Sgc8c with LNA bases and PEG spacers resulted in increased biostability and 2-fold higher affinity than the original aptamers.³⁰ This greater stability makes the LNA-modified Sgc8c aptamer a prime candidate for testing in biomedical applications.

Using this cell-SELEX approach, multiple aptamers for various cell lines have been produced, including aptamers for several types of cancer cells, including lymphocytic leukemia, myeloid leukemia, liver cancer, small cell lung cancer, and nonsmall cell lung cancer.^{12,31} Table 3 summarizes a list of aptamers generated for various cell lines, along with their binding affinity. The aptamers produced can then be modified for certain applications, such as biomarker discovery. Biomarkers that have been targeted by aptamers can be isolated from the cell and analyzed via mass spectrometry.²⁴

2.3. Cell-SELEX for Predefined Targets

As discussed, one of the unique benefits of cell-SELEX is its ability to identify unknown, unique characteristics of a certain cell line. Yet, cell-SELEX also allows for known proteins to be targeted in their native state. By design, the targeted protein can be expressed on the positive cells while the negative cells act as parental mock cells. Cerchia et al. have successfully developed nuclease-resistant aptamers that recognize the human receptor tyrosine kinase RET using this method of cell-SELEX.³² Additionally, Ohuchi et al. developed an aptamer targeting transforming growth factor-beta receptor type III (TbRIII) on the cell surface using this method.³³

Another example of using cell-SELEX to target known protein groups was by Zhang's group while studying HCV. Zhang et al. have also contributed to the field of cell-SELEX. By using whole live cells, an aptamer, ZE₂, targeting the known HCV envelope surface glycoprotein E2 was developed.³⁴ This aptamer may be used to detect the early stages of HCV infection by detecting the HCV surface antigen that is present in sera. It can also target the HCV envelope glycoprotein E₂-expressing cells. Zhang et al. also explain how this aptamer can competitively inhibit E₂ protein binding to CD81, an HCV receptor.

2.4. Hurdles in Cell-SELEX

Because the goal of cell-SELEX is to develop aptamers that target cell-surface markers within biological environments, it is important to use live cells during the selection. Therefore, proper cell culture techniques are imperative. Improper cell culturing techniques can, in turn, cause inadequate aptamer selection. For example, overgrowth of cell culture leads to higher rates of cell death and can potentially lead to alteration in cell morphology and protein expression. Also, cells that have been cultured improperly may develop different levels of expressed proteins. If these cells are used during the selection process, aptamers may target the abnormally expressed proteins, leading to subsets of aptamer families.

The absence of bands after running gel electrophoresis results from the small amount of DNA present. Therefore, the number of cycles and/or the amount of selected pool template can be increased. On the other hand, too much DNA is indicated by the abundance of nonspecific amplicons. In this case, the number of cycles should be increased. The annealing temperature should also be increased while the concentration of primers is lowered.

Although aptamers have successfully targeted a number of cell membrane proteins and cell lines, it remains difficult to develop high-affinity aptamers for some proteins using the standard RNA and DNA. Gold et al. proposed a method for developing aptamers for any protein through SELEX using a new class of aptamers termed "slow off-rate modified

aptamer” (SOMAmer).³⁵ Similar alterations like these may be applied to cell-SELEX. These aptamers increase their chemical diversity by adding protein-like properties to them, such as functional groups that mimic amino acid side chains. By using modified deoxyribonucleotides that incorporate one of four dUTPs modified at the 5'-end and SELEX methods, DNA aptamers could be selected. The efficacy of this system was tested when the modified aptamers were selected against 13 “difficult” human proteins that had previously failed to produce high-affinity aptamers using SELEX with unmodified DNA. The protein GA733-1 was used as a control because it could be selected against unmodified aptamers using SELEX. Only the modified aptamers were selected against these “difficult” proteins with the requisite high affinity. As shown in Table 4, certain modifications worked better than others for proteins, indicating the importance of aptamer modifications and optimization of such modifications in a given protein. The results suggest that modified nucleotides can help aptamers target a much broader range of proteins and improve their binding properties.

3. BIOMARKER DISCOVERY

3.1. Importance of Aptamers in Biomarker Discovery

One of the key pathways to true molecular medicine is through biomarker discovery. Biomarkers indicate a change in the expression or state of proteins, genes, or small molecules under changing physiological conditions or during pathogenesis. By definition, biomarkers provide a quantifiable measurement of biological compounds where the “abnormal” levels are compared to the “normal” levels. This footprint provides an important clue for clinical diagnosis, monitoring, and treatment. Biomarkers can take multiple forms, with the most popular being proteins or unique DNA sequences.³⁶ Irrespective of form, biomarkers must be unique to the disease or cell line. While biomarker discovery is challenging, its potential utility cannot be questioned. Developed biomarkers can be used for an array of purposes, depending upon their occurrence at a specific stage of a disease. For instance, presumed biomarker BRCA1 germline mutation can be used to estimate the risk of developing breast or ovarian cancer, while HER2 expression can be used to predict response to breast cancer therapy.^{37,38} However, it is this very information that also makes biomarker discovery a difficult task. The proteomics of a cell changes throughout pathogenesis, leading to different concentrations of biomarkers at certain stages. This means a vast amount of data needs to be processed from samples progressing through different stages.

However, few biomarkers are used clinically, and the rate of bringing biomarkers to the clinical stage is declining.³⁹ As a consequence of the increasing awareness of the selection process and the ability to use multiplexed microarray systems, researchers should be able to reverse this declining trend by more effectively searching for biomarkers of known diseases by allowing for a wide range of markers to be screened at once. Because genomics and microarray technology are improving with more economical computing power, an infrastructure now exists that allows for a large amount of data to be collected and analyzed at once.

Although a global proteomic reading in serum is able to provide key information for clinicians, the ability to identify a single protein that is indicative of an unhealthy patient is

still the ultimate goal. Current platforms either look for one single biomarker or analyze an array of proteomic ratios to determine a biomarker footprint.

In contrast to mAbs, aptamers are able to target unique properties of cells through their exponential enrichment of ligands, which produces a more specific aptamer pool with each round of selection. This fundamental aspect of selection makes aptamers prime candidates for biomarker discovery. Cell-SELEX selects aptamers against specific cell lines, even when only basic data of the cell's membrane characteristics are available. Thus, the unique properties of these cells can be ascertained by post cell-SELEX analysis to precisely determine the bound molecule. A cell-SELEX-based platform is a significant improvement over the standard systems utilized for biomarker discovery.

Monoclonal antibodies (mAb) have been used to validate single biomarkers by specifically targeting proteins that are significantly expressed in unhealthy cells or tissue. However, monoclonal antibodies require prior knowledge of the targeted protein. Developing cell-specific antibodies for the detection of highly expressed unknown epitopes is nearly impossible by the inherent nature of antibody development.

Specifically, with their ability to distinguish cancer cells from normal cells, aptamers allow a comparative strategy to identify differences at the molecular level and promote the discovery of molecular features of cancer cells. When bound to cell membrane receptors, aptamers provide an effective approach for the discovery of biomarkers as disease signals. In addition, because aptamer probes recognize molecular signatures on the cancer cell surface with high specificity, tumor cell profiles can be defined, perhaps leading to more "personalized" cancer treatment.

3.2. Biomarker Candidates Produced from Cell-SELEX

From analyzing how certain aptamers bind to certain cell lines, relationships between expressed proteins and cell lines may be acquired. For instance, in our first try for targeted protein identification, sgc8 was labeled with a biotin tag, and its binding complex with the target was extracted using streptavidin-coated magnetic beads. By comparison with the control experiments using random DNA, characteristic protein bands on the SDS-PAGE captured by sgc8 were digested and subjected to LC-MS/MS analysis. As a result, a transmembrane receptor, PTK7 (protein tyrosine kinase 7), was identified and verified as the aptamer's target.

A distinct relationship between the overexpression of PTK7 and CCRF-CEM cells (T-ALL) has been observed.⁴⁰ Although the exact function of PTK7 is unknown, its strong correlation with CEM cells warrants further investigation. Interestingly, antibody anti-PTK7 and aptamer sgc8 do not compete for binding; rather, they both bind to PTK7, as indicated by the flow results in Figure 3.⁴⁰

We developed another aptamer targeting Ramos cells that are present in Burkitt's non-Hodgkin's lymphoma (BL) and composed of heterogeneously aggressive malignant B-cells. BL is commonly found in HIV-infected patients and is a serious health concern.⁴¹ BL is associated with the deregulation of the expression of c-myc, a gene coding a basic helix-

loop–helix transcription factor that binds to DNA sequences. C-myc plays a critical role in the transcriptional regulation of downstream genes that control a variety of cellular processes.^{42,43}

From targeting Ramos cells, aptamer TD05 was developed. To determine the cognate target of TD05, the aptamer was chemically modified to covalently cross-link with its target, and streptavidin-coated magnetic beads were used to enrich the target. After using mass spectrometry, the target protein was identified to be an immunoglobulin heavy mu chain (IGHM) molecule.⁴⁴ IGHM is the heavy chain portion of the IgM protein. IgM is a primary component of the B-cell receptor complex expressed in Burkitt's lymphoma.

While cell-SELEX is a powerful tool for targeting unique, unknown characteristics of certain cell lines, it is also important to be able to more effectively target known biomarkers and study them in depth. Cell-SELEX not only allows one to find new extracellular proteins but also allows one to be able to target known proteins on the cell's surface. One such method was utilized in selecting against tenascin-C. Gold et al. used the glioblastoma cell line U251 during selection. Glioblastoma is an aggressive form of cancer and one of upmost concern due to its poor prognosis. After the selection process, Gold et al. were able to identify an aptamer that had a strong binding affinity to an extracellular protein, tenascin-C, found in the tumor matrix.²² Tenascin-C is believed to be involved in embryogenesis and oncogenesis pathways as well as being correlated with malign tumors more than benign tumors.⁴⁵

Other aptamers have been developed for interesting cellular markers. With further research, researchers hope these aptamers will give way to more useful biomarkers. For instance, Schluesener et al. have developed a DNA aptamer that binds to rat brain tumor microvessels. The aptamer is able to bind to microvessels of rat brain glioblastoma but not the vasculature of the normal rat brain including peritumoral areas. After the selection process, it was identified that the aptamer binds to a rat homologue of mouse pigpen, an endothelial protein.²³ The expression of this protein parallels the transition from quiescent to angiogenic phenotypes in vitro. Neoangiogenesis is an important part of tumor development, and the selected aptamer can be used as a probe for analysis of the pathological angiogenesis of glioblastoma.

Biomarkers can be utilized for health concerns other than cancer. Bacteria and virally infected cells can have their own molecular biomarkers. Zhang et al. were able to develop an aptamer for virulent *Mycobacterium tuberculosis*. Tuberculosis (TB) is a global problem that continues to be a major concern. The aptamer developed, NK2, binds to the virulent strain of *M. tuberculosis* (H37Rv) with high affinity and specificity.⁴⁶ This aptamer binds to H37Rv cells without binding to *Mycobacterium bovis*, termed bacillus Calmette–Gue'rin (BCG). As these virally infected cells and bacteria are studied in greater detail, we hope to be able to identify their biomarkers. The authors also found that the aptamer improves CD4⁺T cells to produce IFN- γ after binding to H37Rv.

3.3. Multiplexed Molecular Profiling

Gold et al. have contributed much to the field of proteomics. The group utilizes an array to discover molecular properties in proteomics that are able to transform the complex proteomic samples, that is, plasma, serum, or cell lysates, into a quantifiable protein structure.³⁵ This solution-based array takes advantage of equilibrium binding, as well as the kinetics of binding and dissociation. In solution, the SOMAmers contain biotin, a photocleavable group, and a fluorescent tag. All SOMAmer–protein complexes were captured on streptavidin beads. These beads are washed after being subjected to protein samples to remove unbound proteins. Afterward, UV light irradiation is used to release the complexes from the beads into a high concentration of dextran sulfate, an anionic competitor. The biotin remains a part of the SOMAmer. The anionic competitor disrupts noncognate complexes, allowing only the proteins to contain biotin. A second set of beads is able to recapture these complexes, and uncomplexed proteins are removed by washing. The SOMAmers that remain can be hybridized to complementary probes printed onto a DNA microarray in high pH-denaturing conditions. The difference in dissociation rates between cognate and noncognate interactions is what leads to such specificity.

Despite the advancement of the array platform where 813 proteins were measured from the current array, optimization is still required to provide significant diagnostic results. Gold et al. compared plasma proteomic signatures from 336 women with suspicious mammogram findings. Of these 336, 32 had ductal carcinoma in situ, 57 had invasive breast cancer, and 247 had benign disease. Unfortunately, no statistically significant differences were observed from the results acquired using the 813 protein analysis.

However, the group had more favorable results with chronic kidney disease (CKD). Forty-two samples were subjected to the array testing. Of the 42, 11 had early stage CKD based on estimated glomerular filtration rate (GFR) (eGFR, defined as stages 1–2, median creatinine clearance 70 mL/min/m²), and the other 31 had late-stage CKD (stages 3–5, median creatinine clearance 25 mL/min/m², range 7–49 mL/min/m²).⁴⁷ This method used an array that tested 614 human proteins. Sixty proteins varied significantly between the two groups. Eleven proteins with the highest degree of variation were identified. These proteins further increased their odds of being biomarkers for CKD progression by the inverse correlation between eGFR and protein concentration. These 11 proteins also include two known biomarkers for CKD: cystatin C and β 2 microglobulin (B2M0 β ₂-microglobulin).

To test the cancer cell recognition of cell-SELEX-derived aptamers, 6 aptamers, which were acquired through selection of two leukemia cell lines (Toledo (B-cell ALL) and CCRF-CEM (T-ALL)), were selected.⁴⁸ Using more than 20 related leukemia cell lines and the cells from normal human bone marrow aspirates, all of the aptamers demonstrated excellent recognition of their targets, and combinations of selected aptamers produced distinct patterns for different tumor cells. Therefore, these aptamers were next tested for their ability to characterize real samples from leukemia patients. Three aptamers (sgc8, sgc3, and sgd3) bound selectively to T-ALL patient samples. Moreover, the differential binding of these three aptamers showed the ability of aptamers to distinguish molecular differences among patients with the same diagnosis by current technology. Two aptamers, Sgc4 and sgd2, bound to a high percentage of cells in one leukemia (AML) patient sample, indicating that

this particular patient's cells were expressing surface markers similar to those from patients with T-ALL and B-ALL. These results demonstrate the ability of these aptamers to specifically recognize molecular differences between patients. Correlations between the differential aptamer binding and the specific phenotypes and prognosis of these patients are being investigated.

3.4. Cell Lines That Share Biomarkers

During selection, it is possible to obtain aptamers that also bind to other cancer cell lines. These aptamers may give further insight into biomarker discovery in terms of a more general biomarker that is related to certain cancer cells. For instance, aptamers have been developed to target ovarian cancer. Developing biomarkers that can be detected at an earlier stage of ovarian cancer is needed. The most commonly used serum biomarker for clinical diagnosis and prognosis is ovarian cancer antigen 125 (CA-125). CA-125 value is elevated in approximately 90% of late-stage cases of epithelial ovarian cancer (stages 3 and 4). However, while it is only elevated in 50–60% of women with early stage disease, it is also elevated in a number of benign conditions.^{49–54}

In this work, a total of 13 aptamers were selected for two model ovarian cancer cell lines: the OCCA line TOV-21G (10 aptamers) and the ovarian serous adenocarcinoma line CAOV-3 (3 aptamers).^{28,55} To identify aptamers that specifically bind to ovarian cancer cells, the cervical cancer cell line HeLa was used for counter selection. After 22 rounds of SELEX, an enriched pool that specifically bound to the model OCCA cell line, but only marginally to HeLa cells, was obtained. Thus, the pool was successfully enriched for sequences binding surface markers expressed by the model OCCA cell line, but not by cervical cancer cells.

Sequencing was performed to identify aptamer candidates by generating large quantities of sequences. This number of sequences (here a minimum of 2000 per pool) is large enough to allow identification of aptamers that only have a small representation in the pool (i.e., less than 1%). Table 5 shows that aptamers were present at a stage when only minimal enrichment was observed. Interestingly, the size percentage of AptTOV1 decreased as SELEX progressed. The high affinity of this aptamer would make one think otherwise. This means that even relatively small families can lead to aptamers. These families refer to sequences with the same homology after sequencing has been performed. Ten sequences showing the best homology throughout the pools were selected as aptamer candidates, synthesized, and tested for binding to the model ovarian cancer cell lines. All of the candidates bound to TOV-21G, with binding affinities in the pico- to nanomolar range. Other aptamers seemed to increase in size as enrichment progressed; aptamers aptTOV1 ($K_d = 0.256 \pm 0.08$ nM) and aptTOV2 (0.906 ± 0.25 nM) bound very tightly to TOV-21G cells. Both aptamers could distinguish TOV-21G from HeLa cells. Five of the aptamers selected against TOV-21G showed binding to CEM cells (acute lymphoblastic leukemia), while none of the aptamers bound to Ramos cells (Burkitt's lymphoma) or HL-60 (acute promyelocytic leukemia). All of the obtained aptamers bound to colorectal adenocarcinoma (HCT-116) and glioblastoma (A172). The aptamers obtained from TOV-21G did not bind to DLD-1 (Dukes'

type C colorectal adenocarcinoma), while the aptamers selected against CAOV-3 cells did bind to this cell line.

The targets for these aptamers are most likely downregulated or silenced in these two cell models. Additionally, the AptTOV aptamers show binding to cancer cell lines from unrelated cancers, and some AptTOV aptamers also bound to CEM cells. This result suggests again that the aptamers obtained from this SELEX can be used to profile the expression of membrane proteins of different cancers. Identifying the targets of the selected aptamers is expected to shed light on the underlying mechanisms involved.

To investigate the nature of the target molecule of each aptamer, binding of each aptamer was tested after treatment of the target cells with the proteases trypsin or proteinase K. As indicated in Figure 4a, aptTOV1 shows a clear loss of binding to TOV-21G after protease treatment. The same behavior was also observed with all other AptTOV aptamers. Interestingly, for the second model cell line, CAOV-3, DOV3 and DOV4 retained their binding after protease treatment, suggesting that these aptamers may not bind cell-surface membrane proteins, but rather another type of cell-surface marker, that is, carbohydrate or lipid. Neither DOV3 nor DOV4 bound to the tested leukemia cells. Although AptTOV may not be the most selective aptamer, it still supplies evidence of the pathology in ovarian cancer by identifying characteristics shared by certain cancer cells. AptTOV aptamers neither bind to cancers of specific etiology (CAOV3) nor HeLa. However, these shared membrane characteristics among cancer cell lines may be able to help answer underlying questions about the development of cancer. Interestingly, these aptamers appear to be insensitive to protease digestion. Also, because results show binding to all tested adenocarcinoma cells, but not leukemia cells, further investigation of these underlying differences between cancer types is justified.

Studying the interaction between different aptamers and different cell lines further shows how certain cell lines possess similar characteristics. By using CCRF-CEM (the T-cell acute lymphoblastic leukemia (ALL) cell line) as the target cell line and Ramos (the B-cell line from human Burkitt's lymphoma) as the negative control, 10 aptamers having high affinity for CCRF-CEM cells with calculated equilibrium dissociation constants (K_d) in the nanomolar-to-picomolar range were validated.²¹ These aptamers also performed well in real biological samples, as all of them could recognize their targets with high specificity and affinity and even recognize molecular differences between patient samples (Table 2).

3.5. Difficulties of Biomarker Discovery

Even with an aptamer-based platform for discovering biomarkers and increased computing power available to process large amounts of data obtained, barriers still need to be overcome. First, samples from patients are limited in both quality and quantity for most laboratories. Therefore, proper studies of proteomics across the same platform with the same conditions are difficult to accomplish. These conditional differences are especially difficult to match when analyzing different tissue samples that are acquired from surgery. Furthermore, as mentioned above, levels of proteins for diseases at certain stages can vary dramatically. A cell's proteomic composition changes throughout its life cycle, especially when it is under the influence of a developing disease. At this point, changes are not well

established for specific cell lines. Furthermore, the ratio of the overexpressed protein to the normal levels needs further analysis for a wide range of samples, as current testing methods are time-consuming and labor-intensive. Therefore, to make accurate diagnoses, biomarker expression of a disease needs to be performed at all stages of the disease and with multiple tissue samples. The real utility of biomarker analysis will not be realized until many samples are acquired and tested in a timely manner from a large group of people. Because the human proteomic library consists of approximately 20 000 proteins, plus post-translational variants that span a concentration range of approximately 12 logs, a vast amount of data needs to be tested and examined.

Gold et al. address the second barrier, to a certain degree, with their multiplexed aptamer biomarker discovery platform. The platform is capable of measuring approximately 800 proteins with very low limits of detection (1 pM average), 7 logs of overall dynamic range, and 5% average coefficient of variation.³⁵ This design allows complex protein matrices to be transformed into manageable, quantifiable signatures of aptamer complexes. DNA microarrays are very useful in protein analysis based on their ability to quantify results. Multiplexing allows for the same specificity, but can detect an array of biomarkers, as well as an array of tissue samples. The team studied early stage and late-stage CKD and identified 60 proteins that varied significantly between the two stages. Their unique multiplexing system allows for many proteins and samples to be analyzed rapidly. Similar experiments need to be conducted to bring biomarkers to clinical stage.

A well-developed aptamer-based, multiplexed system will be able to indicate accurate signals for disease progression at the earliest of stages. The ultimate goal of aptamer based biomarker discovery is to utilize a high-throughput system that is able to accurately analyze protein compositions of different cell lines. The data collected from the analysis can then be used to more accurately diagnose cancer at earlier stages.

4. APTAMER-BASED CELL CAPTURE AND DETECTION

Cell recognition and detection are useful for analyzing tissue samples or for capturing circulating tumor cells. By measuring specific cellular levels within the blood, clinicians can judge patients' responses to treatment or predict the probability of the onset of a specific disease. The ability to detect cells at a very low concentration is critical for detecting circulating tumor cells, as most solid tumor cells can be found at concentrations upward of 200 cells/mL in the average adult male (0.004% of cell population in the blood).^{57,58} Generally, in vivo tumors shed only 10^6 tumor cells per gram of tumor tissue per day into the bloodstream.⁵⁹ This small concentration requires high specificity for accurate detection, a requirement unmet with current clinical platforms.

The limit of detection using aptamers varies depending on the platform. Determining the appropriate detection platform for your application is greatly determined by cost and the level of detection that is needed to make an early, reliable reading. For certain tests, this limit of detection may be flexible. However, for detecting CTCs, the greatest sensitivity possible is desired. Sharma et al. utilized an aptamer based electrochemical sensor that is able to detect lung cancer cells with a limit of detection of 10^3 cells/ml within 60 s.⁶⁰ Song et al.

describe an aptamer-based polymerase chain reaction method for cell detection that boasts a limit of detection of 0.13 cells.⁶¹ The pattern recognition of cells method (described below) was used to reach a limit of detection of 10 cells in a 250 μL sample volume.⁶²

4.1. Traditional Platforms of Detection

Previous methods of cell separation, such as dielectrophoresis and sedimentation, rely heavily on physical differences among cells.⁶³ Yet, for separating target cells from matrix cells, physical differences can be negligible, given the differences in certain levels of protein expression. Additionally, fluorescent-activated cell sorting (FACS) often gives homogeneous indication of subpopulations in the sample; however, FACS requires a certain level of expertise for operation and a lengthy time period to label the cells with fluorescent tags, usually through antibody labeling.

For immunophenotypic analyses that use antibody probes, the system can become rather complex because antigens used for the cell-surface detection are generally not exclusively expressed on a given single cell type. This can result in false-positive signals and can influence sensitivity. To decrease the risk of false-positives, immunophenotypic analyses incorporating antibodies must use multiple antibody probes for accurate cell detection.

Another traditional method for cell detection is PCR-based. Although this method has been proven highly sensitive for cell and disease detection,^{64–77} it is, in essence, a method that indirectly detects cells by monitoring RNA expression, thus requiring prolonged RNA isolation before analysis. Additionally, false-negative results can arise, especially when detecting tumor cells in low abundance, based on the variable sensitivity.⁶⁴ As the antibody and PCR-based immunophenotypic systems show, complexity and high cost are factors that have to be considered when performing such tests. Recently, an aptamer-based PCR system has been designed to resolve the shortcomings of traditional PCR-based systems. Song et al. have proposed a platform that uses acute myeloid leukemia (HL-60) cell-specific aptamers in combination with PCR amplification and signal amplification of conjugated polymers to develop a detection system that boasts a single-cell detection limit.⁶¹ Figure 5 illustrates the scheme.

4.2. Magnetic Cell Separation

How aptamers and nanoparticles with magnetic properties could be combined to easily separate specific cells from a given population was investigated.⁶⁷ To take advantage of the magnetic properties of iron oxide, iron oxide-doped silica nanoparticles were used for accurate cell detection and extraction, and fluorescent dyes were incorporated for signaling. To test the feasibility of the system, leukemia cells were chosen as the target cell line. An 88-base oligonucleotide sequence targeting CCRF-CEM acute leukemia cells and possessing a K_d of 5 nM was chosen for the aptamer. This dual-nanoparticle assay, one consisting of aptamer-modified iron oxide-doped silica nanoparticles and the other consisting of aptamer-modified fluorescent dye-doped nanoparticles, allowed for both signaling and extraction. The small size and relatively high surface area of the iron oxide-doped silica nanoparticles provide enhanced extraction capabilities, exceeding those of the commonly used micrometer-sized particles.⁶⁵ The signal intensity corresponding to each aptamer could be

amplified from the dyes doped to the nanoparticles. This system not only boasts a high sensitivity, but also a low time requirement when compared to immunophenotypic- and PCR-based analyses, which both take a few hours to complete, from sample preparation to data collection. Running the samples in the PCR machine alone takes at least 45 min. The dual-nanoparticle system can be completed in less than an hour. Extraction of target cells from whole blood samples has proven to be successful. Control experiments indicated that the aptamer sequence used was stable in serum samples for up to 2 h. Target cells were spiked into whole blood samples (500 μL) and compared to unspiked samples after magnetic extraction to make certain that target cells could be detected in complex biological samples. As shown in Figure 6, nonspecific interactions caused the unwanted collection of some red blood cells, but the lack of RuBpy fluorescent signal on the unwanted cells still allows cells to be accurately distinguished. For magnetic extractions from whole blood samples, 40% of the spiked target cells were routinely recovered after three magnetic washes and after accounting for dilution. This is consistent with current extraction efficiency values reported by immunomagnetic separation.^{68,69}

The utilization of aptamer-conjugated magnetic and fluorescent nanoparticles in this assay was made possible by the presence of sufficient aptamer binding sites for both types of particles on the target leukemia cells. For the analysis of cells having few aptamer recognition sites, different aptamers, or other recognition elements, can be labeled on each type of particle to eliminate competitive binding. This system is now capable of detecting and capturing multiple cell lines in a stepwise manner. Three different aptamers were used to detect and extract cell samples: CEM, Ramos, and Toledo. Figure 7 shows how the three cell samples were extracted and detected by fluorescent imaging using magnetic nanoparticles and dyedoped nanoparticles modified by the three aptamers.

4.3. Magnetic Detection with Profiling Capabilities

Because biomarkers can be present at some level among multiple cancer cell lines, it may be difficult to accurately diagnose a specific disease using just one probe. The expressed proteins are typically found with varying concentrations among cancer cell lines, and they are expressed at different levels at different stages of growth. Fortunately, these proteomic differences may be exploited through the use of aptamers to profile these cells by measuring the intensity of the signal of cell binding from the aptamer.

Aptamer-conjugated magnetic nanoparticles were utilized to create a pattern recognition platform for cancer cells.⁶² These nanoparticles can be used as effective magnetic relaxation switches (MRSw) for the detection of molecular interactions. Because most biological samples exhibit virtually no magnetic background, magnetic relaxation switches can be used for ultrasensitive detection. The use of aptamer-conjugated nano-particles for the collection of cancer cells and subsequent detection using aptamer-conjugated fluorescent nanoparticles (ACFNPs) has been previously reported.^{67,70} This design is the first to use ACFNPs for detection and cell profiling. Figure 8 shows how these nanoparticles can emit different signals based upon the pattern that emerges when different aptamers interact with different cellular membranes.

When the ACMNPs are well dispersed, a high T_2 signal with the surrounding water protons is the result. However, ACMNPs in the presence of the target lines aggregate, decreasing the T_2 of adjacent water protons. The detection scheme is based upon the change of spin-spin relaxation time (ΔT_2) of the surrounding water protons. The clustering of ACMNPs induces the coupling of magnetic spin moment and strong local magnetic fields. The zeta potential (ζ) of this particle increases from -32.4 ± 3.7 mV to -41.8 ± 2.6 mV. Once again, nanomaterials with high surface area allow for more efficient aptamer interaction with the target. This surface area allows for the attachment of multiple aptamers, resulting in multiple interactions between ACMNPs and receptors on the cell surface. This moiety is also good for storage because it is highly stable with no obvious aggregation or precipitation, even after several months of storage at 4 °C.

To confirm that the change in T_2 was the result of specific aptamer-mediated interaction with the targeted cell line, but not nonspecific aggregation of MNPs, TDO5-ACMNPs were also incubated with CCRF-CEM cells as a control, followed by the relaxation time measurements. The percentage change of T_2 ($\% \Delta T_2$) was defined as follows:

$$\% \Delta T_2 = (T_{2\text{nonspiked}} - T_{2\text{sample}}) \times 100 / T_{2\text{nonspiked}}$$

where $T_{2\text{sample}}$ is the average T_2 relaxation time of ACMNPs in the presence of target cells, and $T_{2\text{nonspiked}}$ is the average T_2 relaxation time of ACMNPs in the absence of target cells. The results show that 10 $\mu\text{g/mL}$ was the optimal concentration for the detection of target cells. Additionally, a strong ΔT_2 emission was observed for different media, including FBS, plasma, and blood.

After the proof-of-concept was completed for proper detection and required sensitivity, ACMNPs were used to monitor the interactions of multiple cell lines using an array. The cell lines chosen represented a variety of cancer cells. A normal cell line was chosen as the control with these cell lines: CCRF-CEM, Ramos, K562, DLD1, HCT116, LH86, and HBE135-56E7. The variations in $\% \Delta T_2$ were quite large. These differences are explained by the differences in affinities among the aptamers to their targeted and nontargeted cells. Figure 8 shows the results for the pattern recognition expressed in $\% \Delta T_2$.

By understanding the targets of these aptamers, protein expression of these cancer cell lines can be ascertained. For the $\% \Delta T_2$ experiments, 1000 cells were spiked in PBS and incubated with each ACMNP, followed by T_2 relaxation time measurement. This relaxation time method for pattern recognition allows for a short incubation time and higher specificity in unpurified native samples. This platform provides a practical way to detect cancer cells and profile cells based upon the magnetic relaxation switch design. Once bound to nanoparticles, the aptamers could function and target cells, as well as provide a multivalent effect, resulting in strong interaction with their environment. The platform does not need complicated instrumentation, only a magnetic relaxation instrument.

4.4. Microfluidic-Based Cell Capture

One concern for the dual-nanoparticle assay is that the labeling can possibly influence the analysis of extracted cells. Also, a lack of flow in the system limits the interaction of the samples with the binding agents. However, these limitations can be overcome with a microfluidic device. Thus, to capture rare cells that are in low concentration, an aptamer-modified microfluidic device able to take advantage of these flow principles and capture cells from a large amount of background cells without the need for sample pretreatment was developed.⁵⁸ These microfluidic devices were designed with the goal of enriching rare cells. One such method for enrichment is cell affinity chromatography (CAC). CAC is an attractive method by its ability to elute cells and allow for processing of cell results. Antibody-coated microfluidic devices have been studied; however, aptamer modifications offer a wider range of selected targets and are more suitable for immobilization onto the microfluidic devices. Furthermore, DNA can be stored for an extended period of time and handled in clinical settings with relative ease. Aptamer Sgc8 was covalently bound to a prototype micro-fabricated poly(dimethylsiloxane) (PDMS) device. It was hypothesized that a channel with decreased height would be able to capture more cells based on the higher probability of cells interacting with the aptamer-coated surface.

Images of the initial cell mixture, with target cells stained red and control cells stained green, show that both cell types are uniformly dispersed and at the same concentration (Figure 9B). However, the target cells dominate the population of captured cells, indicating effective and selective cell capture of the aptamer (Figure 9C). By comparing the image pairs taken at 20 s intervals, it is possible to count the number of cells that are captured on the surface over the course of the cell capture assay.

The PDMS device has input and output ports that allow for connections to a syringe pump for reproducible flow rate. The platform was able to perform at >80% capture efficiency with 97% purity when targeting CEM below a flow rate of 200 nL/s. However, the purity decreases to 86% at the slowest measured flow rate, indicating that nonspecific binding increases as flow rates decrease below 150 nL/s. The device was able to capture approximately 50 000 target cells within 6 min from a 50 μ L sample (500 000 cells/h).⁵⁸ By reducing the channel depth and pulsating the cell solutions versus a constant flow, an increase in cell capture efficiency was experienced. The cancer cells that are captured could then be analyzed using a variety of detection platforms. Microfluidic devices are not only efficient and selective but also an inexpensive tool that can be used to detect cells, even at a low concentration. The design detailed above allows for a high surface area-to-volume ratio that increases the collision rate between the target cells and the capture surface. The percentage of captured cells is comparable to devices that utilize antibodies as high-affinity ligands; however, aptamers can be used for a much greater range of cells.^{58,71–85} This device needs to be optimized before being used as a diagnostic method for patients; however, the amount of cells processed by this device can be increased by simply lengthening the channel, increasing the number of channels, or implementing novel channel geometries. This device addresses the enrichment process for detecting rare cells, but it does not address the second major challenge accounting for detection because having a microscope scan the entire microfluidic device is not practical.

A square capillary channel was developed to capture target tumor cells from a floating suspension.⁸⁷ This square capillary has a cross-section length of roughly five cells and is connected via Teflon to a syringe. Aptamers were immobilized on the surface of the capillary via biotin–avidin chemistry. Molecular probes were utilized according to their specificity toward cells and the number of probes available for targeting cancer cells. Antibodies can be an option, but only in a limited number of circumstances, because only a limited number of cancer cell lines have a truly specific antibody able to recognize cell-surface differences.^{57,58} Figure 10 provides a schematic of the square capillary system and immobilization. This simple design requires no fabrication tests and is ready for clinical applications.

As one may assume, the flow rate greatly alters results for the aptamer-capillary platform. A greater flow rate increases the linear velocity of the cells passing through the capillary. If the cells pass too quickly, they will not have enough time to interact with the aptamers, limiting the number that can be captured. Therefore, multiple flow rates were carried out to determine how cell capture efficiency is altered. To image and analyze cell capture efficiency, an Olympus FV500-IX81 confocal microscope was used. At a flow rate of 300 nL/min, 1374 cells were captured; at 600 nL/min, 558 cells were captured; and at 1200 nL/min, 240 cells were captured.⁸⁷ Furthermore, the geometry of the capillary dictates the efficiency. Square capillaries captured about 33% more cells than circular capillaries of comparable diameter and length. This is hypothesized to be because of the higher cross-sectional area of the square capillaries, thus decreasing the linear velocity of the cells.⁸⁸

The capture efficiency was quite high once parameters were optimized. At a flow rate of 20 nL/min, $91.1 \pm 3.5\%$ of CEM cells were captured. Additionally, colon cells were tested to see if the design would work for other cell lines using the same parameters set forth in the work for CEM cell capture. Aptamer KDED2a-3 ($K_d = 29.2$ nM) bound specifically to the DLD-1 cell line. Using this aptamer, $83.6 \pm 5.8\%$ of DLD-1 cells were captured. Aptamer KCHA10 ($K_d = 21.3$ nM) bound to the HCT 116 cell line. Using this aptamer, $97.2 \pm 2.8\%$ of HCT 116 cells were captured in buffer.

For CEM cells, which were spiked in white blood cell/ platelet suspension, cell capture efficiency was higher than for cells at lower concentrations. For cells at a concentration of 1.02×10^5 cells/mL, capture efficiency was 77.2%; however, for concentrations at 3.00×10^4 cells/mL, capture efficiency was only 8.1%. These results indicate the need for preadjusting cell concentrations when performing cell capture/detection experiments.

The results also indicate that this method of testing does not require extensive fabrication prior to testing, nor does it require overly expensive kits. By utilizing the detection platforms discussed above, clinicians may garner more insight into the health of their patients within a relatively short time period. Proper cell detection can limit misdiagnoses and allow clinicians to track the efficacy of certain drug regimens. This platform not only allows for specificity, but it also performs in a timely manner. Furthermore, it requires significantly fewer cells in contrast to other cell detection methods. Flow cytometry requires approximately 10^5 cells, while Western blot analysis requires approximately 10^7 cells.⁸⁹

4.5. Aptamer-Based Chemiluminescence Detection

Chemiluminescence (CL) is a powerful analytical technique that requires no external light source, that is, fluorescence, to produce a signal. Additionally, its simplicity, low cost, and high sensitivity add to its attractiveness. The sensitivity and stability of CL can be further improved through the use of nanomaterials.

Cui's group determined that a CL system incorporating gold colloids with nanoparticles of different sizes could be improved by enhancing the CL of a luminol-H₂O₂ system based on the catalysis of gold nanoparticles.⁹⁰ Qi reported a label-free, aptamer-based chemiluminescence system based on aptamer-conjugated gold nanoparticles (AC-AuNPs) and the catalytic activity of unmodified AuNPs on the luminol-H₂O₂ reaction.⁹¹ When the aptamer binds to its target, it induces aggregation of AuNPs and enhances the luminol-H₂O₂ chemiluminescence reaction (Figure 11). The results proved to be almost 4 orders of magnitude more sensitive than the current AuNPs-based colorimetric method, as thrombin was detected at a concentration as low as 26 fM. Furthermore, CL outperforms enzyme-linked immunosorbent assays (ELISA), because it recorded a limit of detection for the protein R-fetoprotein (AFP) at a concentration of 5 pg/mL.

CL platforms can be utilized with microfluidic chips to detect rare cells. Liu reports this type of setup where an aptamer-based "sandwich" approach is combined with chemiluminescence analysis.⁹² Aptamers were first immobilized onto microfluidic channels to capture and isolate specific cells from a mixture. AuNPs modified with aptamers were then added to trigger a chemiluminescence reaction upon binding with the cells. In a 3 μ L cell mixture, the system was able to detect 30 target cells.

4.6. Improved Detection via Nanomaterials

For detection of cancer cells, it is not only important to have a specific platform, but also one that is very sensitive in its detection. Through advancement in nanomaterials, aptamers can be engineered in ways that improve detection. The predictable structures of aptamers allow for site-specific chemical modification to permit linkage to advanced signaling mechanisms. Aptamers were conjugated with nanomaterials to enhance cancer cell detection.^{58,66,69,93,94} For instance, the density of cell-surface targets for aptamers is not always abundant, especially for cancer cells in the early stages of development. Therefore, multivalent binding versus single-aptamer binding has been studied to increase this signaling. The large surface area and variable sizes allow nanomaterials to serve as multivalent ligand scaffolds. One such multivalent binding platform by multiple aptamers was accomplished using Au-Ag nanorods (NRs), which measured 12 nm \times 56 nm.⁹³

Nanoparticles offer a desirable platform to incorporate aptamers and fluorescent ornaments. By taking advantage of their tunable and homogeneous size, scientists can effectively utilize these nanoparticles for in vitro imaging. Furthermore, the chemistry for linking aptamers to the nanoparticles, as well as chemical modification with fluorescent dyes, is relatively straightforward. Additionally, nanoparticles offer the ability to deliver drugs or other cargo to desired sites.

Gold Nanoparticles—Gold nanoparticles have attracted considerable attention by their low toxicity and solubility in water. Also, gold nanoparticles have unique optical properties, resistance to photo-bleaching, high surface plasmon resonance (SPR), and enhanced absorbance and scattering with high quantum efficiency. Gold nanoparticles certainly have a high potential to be used for in vitro and in vivo diagnostics.^{90,94,95}

Modifying gold nanoparticles with aptamers provides high signaling capability for cellular imaging. By linking a prostate-specific membrane antigen (PSMA) aptamer (A10) to the surface of gold nanoparticles through a DNA complementary linker, a platform was developed for reflectance imaging using confocal microscopy. The gold nanoparticles were able to bind to the target (LNCaP cells) without binding to the nontarget (PC3 cells) after incubation. A 3–5-fold increase in signal was observed for the LNCaP cells, indicating a use for these aptamer-gold nanoparticles for in vitro imaging.⁹⁶

In depth analysis of aptamer conjugated nanomaterials is out of the scope of this Review. Many different groups have contributed greatly to this field, and it is important to note some of the additional nanomaterials that may be linked with aptamers: superparamagnetic iron oxide NPs,⁹⁷ quantum dots,⁹⁸ porous hollow magnetite NPs,⁹⁹ SWNTs,¹⁰⁰ and gold nanopopcorn-attached SWNT.¹⁰¹

5. APTAMERS IN VIVO

5.1. Imaging

On the basis of the ability of aptamers to recognize certain molecular characteristics, they may be used in advanced imaging after certain modifications. Aptamers by themselves do not have any inherent imaging properties. Therefore, they must be labeled directly with fluorophores, or they can be conjugated with imaging agents, such as iron oxide nanoparticles. Fortunately, aptamers can be chemically modified relatively easily. Researchers have shown interest in further studying these modified aptamers for in vivo molecular imaging by their ability to penetrate deeply into tissue. One such chemical modification allows for aptamers to be used in fluorescence imaging. Fluorescence imaging continues to gain popularity as probes improve and instruments become more sensitive. The general mechanism for fluorescence imaging accounts for fluorophores that absorb photons and re-emit them at a different wavelength. Although fluorescence imaging may not be suitable for use in deep tissue imaging, depth penetrations are improving, and current ranges are in the micrometers to centimeters.^{102,103}

Fluorescent dyes may be synthesized to either the 5' or the 3' ends of aptamers via phosphoramidite chemistry. For in vivo imaging using these fluorescently labeled dyes, the aptamer will circulate until finding the desired target. Upon target recognition, it will bind and emit fluorescence when an external source is added to provide the needed photons. As single aptamers circulate, they emit a very low fluorescence. However, as aptamers become more concentrated, the fluorescence is increased greatly. By identifying areas with high fluorescence, clinicians can determine the locations of the targeted cell line. To further increase fluorescence signaling, multiple dyes may be synthesized to a given aptamer using biotin and streptavidin chemistry.¹⁰⁴

Aptamers were first introduced as imaging probes for in vivo studies in 1997, when a group from NeXstar Pharmaceuticals used a technetium-99m (^{99m}Tc)-labeled aptamer selected against human neutrophil elastase to image inflammation.¹⁰⁵ This aptamer probe showed a higher signal-to-background ratio (S/B) than its antibody counterpart, demonstrating the potential application of aptamers as imaging probes for in vivo studies.

5.2. Instrument Assisted Imaging

Confocal microscopy, fluorescent microscopy, and flow cytometry are all instruments that may be used to image fluorescence (Figure 12). However, these instruments are mostly used for in vitro imaging and are typically used to determine if aptamers have successfully bound to their targets.^{11,14,21,31,32}

To effectively use aptamers for in vivo imaging, the aptamer will be more successful if linked with nanoparticles to obtain greater signaling upon deeper tissue penetration. Nanoparticles may be synthesized to be more suitable for a given instrument.

Magnetic resonance imaging (MRI) is a noninvasive process that allows for the imaging of deep tissue. Mechanistically, it can be compared to nuclear magnetic resonance, but on a scale used for biomedical imaging. MRI takes advantage of the proton relaxation times within tissue to create a contrast gradient. Aptamers linked with contrast agents may create a higher difference in relaxation time, while, at the same time, targeting cell-surface markers.^{106–108} Such imaging agents may be iron oxide nanoparticles or gadolinium-based nanoparticles.¹⁰⁹

Positron electron tomography (PET) and single photon emission computed tomography (SPECT) are two areas of interest for further aptamer development. These two techniques have subcentimeter resolution, while observing molecular interactions, biodistribution, and pharmacodynamics.¹¹⁰ PET requires a short-lived positron emitter, while SPECT requires a gamma emitter. Previous studies suggest that aptamers may be labeled with ^{18}F for PET imaging on the basis of experiments using antisense oligonucleotides labeled with ^{18}F for imaging of gene and mRNA expression.¹¹¹ Antisense oligonucleotides are not considered aptamers, but from a chemical perspective, there should be no reason aptamers cannot be used in such applications.

Impressive experiments have been carried out with in vivo imaging that incorporates aptamers and SPECT. While platforms reported in the literature are slightly different, each shows rapid blood clearance of aptamers, while still being able to accumulate at the tumor site. For SPECT projects, aptamers are conjugated with ^{99m}Tc . One such project used an aptamer selected against tenascin-c (TTA1) and was labeled with rhodamine red and ^{99m}Tc . The experiment studied aptamer uptake and biodistribution in MDA-MB-436 breast cancer cells. Within 10 min, accumulation was detected within the tumor site, and within 3 h, the aptamer was diffused throughout the tumor. The aptamer was cleared by renal and hepatic pathways.¹¹²

5.3. Biosensors

Biological sensors offer sensitive information for a particular cellular environment, and they are gaining much wider recognition by offering smaller, but more sensitive, platforms. More complex aptamer-based biosensors have the ability to recognize small molecules with high sensitivity. As technology improves and drug therapy focuses more on targeting single-molecules, an aptamer sensor that focuses on a micro versus macro scale is certainly needed.

Aptamers derived from cell-SELEX have been studied for their possible use in cancer cell detection. The possibility of using these aptamers for cell detection from an *in vitro* aspect has been discussed in this Review; however, *in vivo* detection should also be a clear goal for researchers, particularly because the ability of aptamers to detect rare cancer cells *in vitro* has been shown. These moieties come in a variety of designs and will certainly evolve. Many aptamers used for sensing rely on fluorescence imaging.

Sensing moieties that can effectively sense intracellular communication, or the levels of certain chemicals near cells and their secretion dynamics, will provide valuable information for developing drugs and better understanding the interactions between cells. These aptamer platforms are also able to provide information relevant to kinetics. Currently, however, scientists cannot solve many detection problems related to intracellular environment or cell-cell communication in real time. Current schemes for monitoring cellular communication usually require complex steps that alter the full functionality of the cells. For instance, enzyme-linked immunosorbent assays (ELISA) or flow cytometry require various steps of washing or staining, altering native cellular conditions. These alterations make it impossible to determine the whole scope of the cell's environment in real time.

For molecular imaging, probes have been designed to be activated in the presence of cancer-specific microenvironments.^{113–121} Two key principles need to be present to have a sensor: a target of interest and signal transduction. This signal transduction is operated by some type of switch. As aptamers bind to the target, they induce a conformational change that acts as that switch. To take advantage of this conformational change, a quencher and fluorescent dye may be used for the signal transduction pathway. This design typically takes the form of a hairpin structure where each strand of the stem either has a fluorescent dye or a quencher. In the absence of target, the hairpin structure is intact, and thus no signal is emitted. However, when the target is present, the aptamer with a hairpin structure binds to its target and goes through a conformational change, allowing the fluorescent dye to be displaced from the dye and emit a signal. This design has been termed activatable aptamer probe (AAP).¹²²

Shi et al. proposed a design where AAPs may be used for enhanced *in vivo* imaging of cancer cells. Figure 13 represents the scheme. This system combines molecular imaging capability with a highly selective sensing platform. Furthermore, this system has a relatively low signal-to-background ratio. As compared to an aptamer *sgc8* that is labeled with a Cy5 label and, hence, “always on”, the signal-to-background ratio was enhanced approximately 2.5 times using the AAP design.¹²²

This AAP design also has a low limit of detection. Using sgc8 as its aptamer and CCRF-CEM cells as its target, the limit of detection in 200 μL was 79 cells by flow cytometry (Figure 14). For further investigation of the design, the AAP was used to see how it reacted to samples that had target and nontarget cells. Therefore, the CCRF-CEM cells were mixed with Ramos cells with ratios of CCRF-CEM:Ramos cells of 9:1 to 1:9. Here, the signals changed from 70.36% to 14.91%.

5.3.1. Sensing Platforms—Previously generated probes that were used to recognize either certain cells or aggregates incorporated an “always on” technique where these probe would increase the intensity of the signal when the probes accumulated.¹²³ This design has been incorporated for a certain number of sensors, such as radioactive, magnetic, and fluorescent agents.^{13,57,108,112,124,125}

5.3.2. FRET Sensor—Aptamer sensors typically use either a fluorescence resonance energy transfer (FRET) or a quencher system. FRET systems are typically made up of two dyes: Cy3 and Cy5. The Cy3 is the donor, and the Cy5 is the acceptor. Therefore, on a fluorescence graph after the sensing has been performed, a decrease in fluorescence from Cy3 and an increase in fluorescence from Cy5 can be seen. This change in fluorescence results from the transfer of the fluorescent energy from Cy3 to Cy5. To transfer this energy, the dyes must be close enough, typically 10–100 Å.¹²⁶ For aptamers, conformational changes usually occur when the aptamer binds with its target. Therefore, the aptamer may be designed in such a way that the dyes are brought into closer proximity after this binding occurs.

5.3.3. Quench Sensor—A quench sensor platform is similar to a FRET sensor in that it involves two molecules whose fluorescence is based upon their proximity. The system usually involves the fluorophore FAM and a quencher such as Dabcyl. When the molecules are far enough apart, the FAM emits distinct fluorescence. When the molecules are close enough, the Dabcyl quenches the fluorescence of the FAM molecule, indicating a signal. This signal results from a conformational change in the aptamer after it has bound to its target, bringing the FAM and Dabcyl molecules together.

As biosensors become more complex, aptamers need to be utilized for sensing the presence of cells, as well as providing more insight into cellular environments.

The use of aptamers for biosensors in complex environments looks promising. The ability of aptamers to detect specific cells within an environment that is diverse, along with their small size, will certainly make for interesting research for many years and, hopefully, translational clinical applications in the not too distant future.

5.4. Degradation of Aptamers

One critical concern when transitioning aptamers to clinical application is their susceptibility to degradation when submitted to in vivo conditions. Aptamers are prone to nuclease degradation in serum, leading to a lower half-life. Limitations such as low biocompatibility and biophysical and chemical instability have prevented the full realization of aptamer delivery in vivo. Furthermore, the small size of aptamers forces them to be subjected to renal

clearance within minutes. By attaching to 40 kDa polyethylene glycol, clearance can be slowed.¹²⁷ By modifying aptamers with functional groups, altering their geometric structure, or encapsulating them, we can significantly increase the amount of time aptamers are able to circulate in vivo.

Protecting aptamers from nuclease degradation is a valid concern. Fortunately, as moieties improve, aptamers become more resistant to degradation to allow for sufficient circulation time within the body to carry out their purpose. This can be accomplished in a variety of ways. One profound leap forward is using xeno nucleic acids (synthetic nucleic acids). These nucleic acids differ by changing specific sugars to chemically create nucleic acids that are still able to store information. Because enzymes are highly specific, they only recognize DNA and RNA for degradation.

Also, by conjugating aptamers with high molecular weight polymers, that is, polyethylene glycol¹²⁸ and cholesterol,¹²⁹ aptamers might improve their biostability. This conjugation has also been shown to slow renal filtration rates, thus increasing the half-life of circulating aptamers. When protecting aptamers, one must also take into consideration biocompatibility and toxicity. These restrictions have limited the full potential of aptamers to be used for in vivo applications. By noncovalent physical adsorption or covalent interactions, aptamers may be conjugated to carbon nanotubes, subsequently increasing their stability and binding affinity.¹³⁰ While other methods are used on the basis of an encapsulation technique using silica, polymers, or gels, these are usually engineered for drug delivery.^{131–133}

Nucleic acids outside of the traditional nucleic bases, particularly locked nucleic acid (LNA), were studied to see if they can improve traditional aptamers. LNAs are similar to traditional bases, but they have a methylene bridge connecting 2'-oxygen of the ribose with 4'-carbon.^{134,135} Figure 15 depicts the structure of LNAs. The group incorporated LNA into molecular beacons. As compared to regular molecular beacons, the LNA molecular beacons possessed a 25-fold enhancement in fluorescence signaling. The LNA molecular beacons also possessed greater stability.¹³⁶ These molecular beacons can be used as effective biosensors.

Improving the stability of oligonucleotides has been an ongoing issue. By making modifications on the 2' position of ribonucleotides or the phosphodiester backbone, the enzymatic degradation of the oligonucleotide can be slowed. Many chemical modifications such as this have been attempted, such as the ones that follow: 2'-aminopyrimidine,¹³⁷ 2'-*O*-methylpurine, 2'-fluoropyrimidine, and 5-(1-pentynyl)-2'-deoxyuridine.

6. CONCLUSION

Aptamers possess a unique set of attributes that allows them to be used for a variety of applications in cellular analysis. Through the process of cell-SELEX, aptamers may be selected with high selectivity and specificity toward a targeted cell line. Not only can aptamers bind to certain molecules with high affinity, they can also be chemically modified with relative ease, allowing researchers to continue pushing this field further. It is not surprising that aptamers continue to warrant such great interest two decades after their

development. As nanotechnology improves with instrumentation, aptamers will continue to improve in function. However, even though aptamers are popular among different research fields, their use in commercial areas is limited. From a drug development perspective, further optimization is needed to improve stability and half-life within a patient. Yet, in terms of analytics, aptamers surely have a place, especially for in vitro applications. Furthermore, their use in biomarker discovery and imaging will greatly enhance molecular medicine. As explained above, cell-selected aptamers are able to recognize subtle differences among cellular membranes. These differences can be exploited for cell detection, capture, and imaging. One of the most promising features of aptamers is their role in biomarker discovery. Currently, aptamer-based platforms are the most efficient and effective platforms for analyzing a wide range of cell lines. Multiplexed systems are able to deliver insight into cellular traits among different cell lines. These traits will substantially assist researchers in the targeting of diseases as complex as cancer.

Acknowledgments

This work is supported by grants awarded by the National Key Scientific Program of China (2011CB911000), NSFC (21025521), the Foundation for Innovative Research Groups of NSFC (Grant 21221003), China National Instrumentation Program 2011YQ03012412 and by the National Institutes of Health (GM079359 and CA133086).

Biographies



Dr. Weihong Tan, Distinguished Professor of Chemistry and Professor of Physiology and Functional Genomics, earned his Ph.D. (1993) from the University of Michigan. Dr. Tan's research interest is in Chemical Biology and Bioanalytical Chemistry. His group developed the cell-SELEX technique to screen nucleic acid aptamers for specific recognition of diseased living cells. They further use these aptamers for identification of diseased-associated biomarkers, laboratory investigation of early disease diagnosis, targeted drug delivery, and cancer cell enrichment and separation. In addition, using DNA and other nanomaterials as building blocks, Tan's group have engineered a variety of DNA nanostructures to be used as drug carriers, biosensors, and nanomotors for energy harvesting.



Michael J. Donovan joined the Tan Research Group at the University of Florida in the year 2008, as an undergraduate. He received his B.S. in chemistry, with emphasis on biochemistry, from the University of Florida in the year 2011. He is currently pursuing his graduate studies at Hunan University, China. Donovan's research interests include aptamer applications, cancer therapy, molecular diagnostics, and drug delivery.



Jian-Hui Jiang obtained his Ph.D. in analytical chemistry in 1999 from Hunan University, and then began his academic career at the same university. From 2000 to 2001, he had postdoctoral study at Kwansai Gakuin University (Japan). He has been a full professor since 2003 at the State Key Laboratory for Chemo/Biosensing and Chemometrics, College of Chemistry and Chemical Engineering in Hunan University. He is a winner of the Outstanding Young Scientist Fund from NSFC, and has published over 100 papers in his major research areas including biosensors, bioanalytical chemistry, and chemometrics.

References

1. Santoni V, Molloy M, Rabilloud T. *Electrophoresis*. 2000; 21:1054. [PubMed: 10786880]
2. Mirza SP, Halligan BD, Greene AS, Olivier M. *Physiol. Genomics*. 2007; 30:89. [PubMed: 17341690]
3. Wu CC, Yates JR III. *Nat. Biotechnol.* 2003; 21:262. [PubMed: 12610573]
4. Anderson NL, Anderson NG, Haines LR, Hardie DB, Olafson RW, Pearson TWJ. *Proteome Res.* 2004; 3:235.
5. Kang WJ, Chae JR, Cho YL, Lee J, Kim S. *Small*. 2009; 22:2519.
6. Ellington A, Szostak J. *Nature*. 1990; 346:818. [PubMed: 1697402]
7. Tuerk C, Gold L. *Science*. 1990; 249:505. [PubMed: 2200121]
8. Patel DJ, Suri AK, Jiang L, Fan P, Kumar RA, Nonin S. *J. Mol. Biol.* 1997; 272:645. [PubMed: 9368648]
9. Mairal T, Özalp VC, Sánchez PL, Mir M, Katakis I, O'Sullivan CK. *Anal. Bioanal. Chem.* 2008; 390:989. [PubMed: 17581746]
10. Jenison RD, Gill SC, Pardi A, Polisky B. *Science*. 1994; 263:1425. [PubMed: 7510417]
11. Bunka DHJ, Stockley PG. *Nat. Rev. Microbiol.* 2006; 4:588. [PubMed: 16845429]
12. Sefah K, Tang ZW, Shangguan DH, Chen H, Lopez-Colon D, Li Y, Parekh P, Martin J, Meng L, Phillips JA, Kim YM, Tan WH. *Leukemia*. 2009; 23:235. [PubMed: 19151784]

13. Hwang, dW, Ko, HY., Lee, JH., Kang, H., Ryu, SH., Song, IC., Lee, DS., Kim, S. J. Nucl. Med. 2010; 51:98. [PubMed: 20008986]
14. Shangguan D, Meng L, Cao ZC, Xiao Z, Fang X, Li Y, Cardona D, Witek RP, Liu C, Tan W. Anal. Chem. 2008; 80:721. [PubMed: 18177018]
15. Ferreira CS, Matthews CS, Missailidis S. Tumour Biol. 2006; 27:289. [PubMed: 17033199]
16. Lupold SE, Hicke BJ, Lin Y, Coffey DS. Cancer Res. 2002; 62:4029. [PubMed: 12124337]
17. Gutsaeva DR, Parkerson JB, Yerigenahally SD, Kurz JC, Schaub RG, Ikuta T, Head CA. Blood. 2011; 117:727. [PubMed: 20926770]
18. Townshend B, Aubry I, Marcellus RC, Gehring K, Tremblay ML. ChemBioChem. 2010; 11:1583. [PubMed: 20572251]
19. Dwivedi HP, Smiley RD, Jaykus LA. Appl. Microbiol. Biotechnol. 2010; 87:2323. [PubMed: 20582587]
20. Li S, Xu H, Ding H, Huang Y, Cao X, Yang G, Li J, Xie Z, Meng Y, Li X, Zhao Q, Shen B, Shao N. J. Pathol. 2009; 218:327. [PubMed: 19291713]
21. Shangguan D, Li Y, Tang Z, Cao Z, Chen H, Mallikaratchy P, Sefah K, Yang C, Tan W. Proc. Natl. Acad. Sci. U.S.A. 2006; 103:11838. [PubMed: 16873550]
22. Daniels DA, Chen H, Hicke BJ, Swiderek KM, Gold L. Proc. Natl. Acad. Sci. U.S.A. 2003; 100:15416. [PubMed: 14676325]
23. Blank M, Weinschenk T, Priemer M, Schluesener H. J. Biol. Chem. 2001; 276:16464. [PubMed: 11279054]
24. Berezovski MV, Lechmann M, Musheev MU, Mak TW, Krylov SN. J. Am. Chem. Soc. 2008; 130:9137. [PubMed: 18558676]
25. Sefah K, Shangguan D, Xiong X, O'Donoghue MB, Tan W. Nat. Protoc. 2010; 5:1169. [PubMed: 20539292]
26. Tang Z, Parekh P, Turner P, Moyer RW, Tan W. Clin. Chem. 2009; 55:813. [PubMed: 19246617]
27. Bast RC Jr, Jacobs I, Berchuck A. J. Natl. Cancer Inst. 1992; 84:556. [PubMed: 1556762]
28. Hasegawa H, Taira KI, Sode K, Ikebukuro K. Sensors. 2008; 8:1090. [PubMed: 27879754]
29. Müller J, Wulffen B, Pöttsch B, Mayer G. ChemBioChem. 2007; 8:2223. [PubMed: 17990265]
30. Kim Y, Cao Z, Tan W. Proc. Natl. Acad. Sci. U.S.A. 2008; 105:5664. [PubMed: 18398007]
31. Tang Z, Shangguan D, Wang K, Shi H, Sefah K, Mallikaratchy P, Chen HW, Li Y, Tan W. Anal. Chem. 2007; 79:4900. [PubMed: 17530817]
32. Cerchia L, Duconge F, Pestourie C, Boulay J, Aissouni Y, Gombert K, Tavitian B, de Franciscis V, Libri D. PLoS Biol. 2005; 3:123.
33. Ohuchi SP, Ohtsu T, Nakamura Y. Biochimie. 2006; 88:897. [PubMed: 16540230]
34. Chen F, Hu Y, Li D, Chen H, Zhang XL. PLoS One. 2009; 4:8142.
35. Gold L, Ayers D, Bertino J, Bock C, Bock A, Brody EN, Carter J, Dalby AB, Eaton BE, Fitzwater T, Flather D, Forbes A, Foreman T, Fowler C, Gawande B, Goss M, Gunn M, Gupta S, Halladay D, Heil J, Heilig J, Hicke B, Husar G, Janjic N, Jarvis T, Jennings S, Katilius E, Keeney TR, Kim N, Koch TH, Kraemer S, Kroiss L, Le N, Levine D, Lindsey W, Lollo B, Mayfield W, Mehan M, Mehler R, Nelson SK, Nelson M, Nieuwlandt D, Nikrad M, Ochsner U, Ostroff RM, Otis M, Parker T, Pietrasiewicz S, Resnicow DI, Rohloff J, Sanders G, Sattin S, Schneider D, Singer B, Stanton M, Sterkel A, Stewart A, Stratford S, Vaught JD, Vrkljan M, Walker JJ, Watrobka M, Waugh S, Weiss A, Wilcox SK, Wolfson A, Wolk SK, Zhang C, Zichi D. PLoS One. 2010; 5:15004.
36. Henry NL, Hayes DF. Mol. Oncol. 2012; 6:140. [PubMed: 22356776]
37. Easton DF, Ford D, Bishop DT. Am. J. Hum. Genet. 1995; 56:265. [PubMed: 7825587]
38. Bang YJ, Van Cutsem E, Feyereislova A, Chung HC, Shen L, Sawaki A, Lordick F, Ohtsu A, Omuro Y, Satoh T, Aprile G, Kulikov E, Hill J, Lehle M, Ruschhoff J, Kang YK. Lancet. 2010; 376:687. [PubMed: 20728210]
39. Gutman S, Kessler LG. Nat. Rev. Cancer. 2006; 6:565–571. [PubMed: 16794639]
40. Shangguan D, Cao Z, Meng L, Mallikaratchy P, Sefah K, Wang H, Li Y, Tan W. J. Proteome Res. 2008; 7:2133. [PubMed: 18363322]

41. Thomas MD, Srivastava B, Allman D. *Cell Immunol.* 2006; 239:92. [PubMed: 16797504]
42. Cambier JC, Campbell KS. *FASEB J.* 1992; 6:3207. [PubMed: 1397843]
43. Trujillo MA, Jiang SW, Tarara JE, Eberhardt NL. *DNA Cell Biol.* 2003; 22:513. [PubMed: 14565868]
44. Mallikaratchy P, Tang Z, Kwame S, Meng L, Shangguan D, Tan W. *Mol. Cell. Proteomics.* 2007; 6:2230. [PubMed: 17875608]
45. Mackie EJ, Chiquet-Ehrismann R, Pearson CA, Inaguma Y, Taya K, Kwarada Y, Sakakura T. *Proc. Natl. Acad. Sci. U.S.A.* 1989; 84:4621.
46. Chen F, Zhou J, Fengling L, Mohammed A-B, Zhang X-L. *Biophys. Res. Commun.* 2007; 357:743.
47. Stevens LA, Coresh J, Greene T, Levey AS. *N. Engl. J. Med.* 2006; 354:2473. [PubMed: 16760447]
48. Shangguan D, Cao Z, Li Y, Tan W. *Clin. Chem.* 2007; 53:1153. [PubMed: 17463173]
49. Hartge PJ. *Natl. Cancer Inst.* 2010; 102:3.
50. Nosov V, Su F, Amneus M, Birrer M, Robins T, Kotlerman J, Reddy S, Farias-Eisner R. *Am. J. Obstet. Gynecol.* 2009; 200:639. [PubMed: 19285648]
51. Munkarah A, Chatterjee M, Tainsky MA. *Curr. Opin. Obstet. Gynecol.* 2007; 19:22. [PubMed: 17218847]
52. Maines-Bandiera S, Woo MM, Borugian M, Molday LL, Hii T, Gilks B, Leung PC, Molday RS, Auersperg N. *Int. J. Gynecol. Cancer.* 2010; 20:16. [PubMed: 20130498]
53. Oaknin A, Barretina P, Perez X, Jimenez L, Velasco M, Alsina M, Brunet J, Germà JR, Beltran M. *Int. J. Gynecol. Cancer.* 2010; 20:87. [PubMed: 20130507]
54. Jacobs IJ, Menon U. *Mol. Cell. Proteomics.* 2004; 3:355. [PubMed: 14764655]
55. Provencher DM, Lounis H, Champoux L, Tetrault M, Manderson EN, Wang JC, Eydoux P, Savoie R, Tonin PN, Mes-Masson AM. *In Vitro Cell. Dev. Biol.: Anim.* 2000; 36:357. [PubMed: 10949993]
56. Van Simaey D, Lopez-Colon D, Sefah K, Sutphen R, Jimenez E, Tan W. *PLoS One.* 2010; 5:13770.
57. Xu Y, Phillips JA, Yan J, Li Q, Fan ZH, Tan W. *Anal. Chem.* 2009; 81:7436. [PubMed: 19715365]
58. Phillips JA, Xu Y, Xia Z, Fan ZH, Tan W. *Anal. Chem.* 2009; 81:1033. [PubMed: 19115856]
59. Barok M, Balazs M, Nagy P, Rakosy Z, Treszl A, Toth E, Juhasz I, Park JW, Isola J, Vereb G, Szollosi J. *Cancer Lett.* 2008; 260:198. [PubMed: 18096313]
60. Sharma R, Agrawal VV, Sharma P, Varshney R, Sinha RK, Malhotra BD. *J. Phys.: Conf. Ser.* 2012; 358:012001.
61. Song J, Lv F, Yang G, Liu L, Yang Q, Wang S. *Chem. Commun.* 2012; 48:7465.
62. Bamrungsap S, Chen T, Shukoor MI, Chen Z, Sefah K, Chen Y, Tan W. *ACS Nano.* 2012; 6:3974. [PubMed: 22424140]
63. Pappas D, Wang K. *Anal. Chim. Acta.* 2007; 601:26. [PubMed: 17904469]
64. Ghossein RA, Bhattacharya S. *Eur. J. Cancer.* 2000; 36:1681. [PubMed: 10959054]
65. Inuma H, Okimaga K, Adachi M, Suda K, Sekine T, Sakagawa K, Baba Y, Tamura J, Kumagai H, Ida A. *Int. J. Cancer.* 2000; 89:337. [PubMed: 10956407]
66. Liu Yin JA, Grimwade D. *Lancet.* 2002; 360:160. [PubMed: 12126839]
67. Herr J, Smith J, Medley C, Shangguan D, Tan W. *Anal. Chem.* 2006; 78:2918. [PubMed: 16642976]
68. Stanciu LA, Shute J, Holgate ST, Djukanovic RJ. *Immunol. Methods.* 1996; 189:107.
69. Benez A, Geiselhart A, Handgretinger R, Schiebel U, Fierlbeck G. *J. Clin. Lab. Anal.* 1999; 13:229. [PubMed: 10494132]
70. Smith JE, Medley CD, Tang Z, Shangguan D, Lofton C, Tan W. *Anal. Chem.* 2007; 79:3075. [PubMed: 17348633]
71. Cheng X, Irimia D, Dixon M, Sekine K, Demirci U, Zamir L, Tompkins RG, Rodriguez W, Toner M. *Lab Chip.* 2007; 7:170. [PubMed: 17268618]
72. Wang K, Marshall MK, Garza G, Pappas D. *Anal. Chem.* 2008; 80:2118. [PubMed: 18288818]

73. Plouffe BD, Njoka DN, Harris J, Liao J, Horick NK, Radisic M, Murthy SK. *Langmuir*. 2007; 23:5050. [PubMed: 17373836]
74. Plouffe BD, Radisic M, Murthy SK. *Lab Chip*. 2008; 8:462. [PubMed: 18305866]
75. Du Z, Colls N, Cheng KH, Vaughn MW, Gollahon L. *Biosens. Bioelectron*. 2006; 21:1991. [PubMed: 16242927]
76. Du Z, Cheng KH, Vaughn MW, Collie NL, Gollahon LS. *Biomed. Microdevices*. 2007; 9:35. [PubMed: 17103049]
77. Zheng T, Yu H, Alexander CM, Beebe DJ, Smith LM. *Biomed. Microdevices*. 2007; 9:611. [PubMed: 17516171]
78. Wojciechowski JC, Narasipura SD, Charles N, Mickelsen D, Rana K, Blair ML, King MR. *Br. J. Hamaetol*. 2008; 140:673.
79. Narasipura SD, Wojciechowski JC, Charles N, Liesveld JL, King MR. *Clin. Chem*. 2008; 54:77. [PubMed: 18024531]
80. Nagrath S, Sequist LV, Maheswaran S, Bell DW, Irimia D, Ulkus L, Smith MR, Kwak EL, Digumarthy S, Muzikansky A, Ryan P, Balis UJ, Tompkins RG, Haber DA, Toner M. *Nature*. 2007; 450:1235. [PubMed: 18097410]
81. Maheswaran S, Sequist LV, Nagrath S, Ulkus L, Brannigan B, Collura CV, Inserra E, Diederichs S, Iafrate JA, Bell DW, Digumarthy S, Muzikansky A, Irimia D, Settleman J, Tompkins RG, Lynch TJ, Toner M, Haber DA. *N. Engl. J. Med*. 2008; 359:366. [PubMed: 18596266]
82. Wolf M, Zimmermann M, Delamarche E, Hunziker P. *Biomed. Microdevices*. 2007; 9:135:141.
83. Murthy SK, Sin A, Tompkins RG, Toner M. *Langmuir*. 2004; 20:11649. [PubMed: 15595794]
84. Sin A, Murthy SK, Revzin A, Tompkins RG, Toner M. *Biotechnol. Bioeng*. 2005; 91:816. [PubMed: 16037988]
85. Kwon KW, Choi SS, Lee SH, Kim B, Lee SN, Park MC, Kim P, Hwang SY, Suh KY. *Lab Chip*. 2007; 7:1462.
86. Chang WC, Lee LP, Liepmann D. *Lab Chip*. 2005; 5:64. [PubMed: 15616742]
87. Martin JA, Phillips JA, Parekh P, Sefah K, Tan W. *Mol. BioSyst*. 2011; 7:1720. [PubMed: 21424012]
88. Ming F, Eisenthal R, Whish WJD, Hubble J. *Enzyme Microb. Technol*. 2000; 26:216. [PubMed: 10689080]
89. Lee H, Yoon T, Figueiredo J, Swirski FK, Weissleder R. *Proc. Natl. Acad. Sci. U.S.A.* 2009; 106:12459. [PubMed: 19620715]
90. Zhang ZF, Cui H, Lai CZ, Liu LJ. *Anal. Chem*. 2005; 77:3324. [PubMed: 15889925]
91. Qi YY, Li BX. *Chem.-Eur. J*. 2010; 17:1642. [PubMed: 21268167]
92. Liu W, Wei H, Lin Z, Mao S, Lin J-M. *Biosens. Bioelectron*. 2011; 28:438. [PubMed: 21856143]
93. Huang Y, Chang H, Tan W. *Anal. Chem*. 2008; 80:567. [PubMed: 18166023]
94. Medley C, Smith J, Tang Z, Wu Y, Bamrungsap S, Tan W. *Anal. Chem*. 2008; 80:1067. [PubMed: 18198894]
95. Huang X, El-Sayed IH, Qian W, El-Sayed MA. *J. Am. Chem. Soc*. 2006; 128:2115. [PubMed: 16464114]
96. Javier DJ, Nitin N, Levy M, Ellington A, Richards-Kortum R. *Bioconjugate Chem*. 2008; 19:1309.
97. Yu MK, Kim D, Lee IH, So JS, Jeong YY, Jon S. *Small*. 2011; 7:2241. [PubMed: 21648076]
98. Li J, Xu M, Huang H, Zhou J, Abdel-Halimb ES, Zhang JR, Zhu JJ. *Talanta*. 2011; 85:2113. [PubMed: 21872066]
99. Chen T, Shukoor MI, Wang R, Zhao Z, Yuan Q, Bamrungsap S, Xiong X, Tan W. *ACS Nano*. 2011; 5:7866. [PubMed: 21888350]
100. Zhu Z, Tang Z, Phillips JA, Yang R, Wang H, Tan WJ. *Am. Chem. Soc*. 2008; 130:10856.
101. Beqa L, Fan Z, Singh AK, Senapati D, Ray PC. *ACS Appl. Mater. Interfaces*. 2011; 3:3316. [PubMed: 21842867]
102. Weissleder R, Pittet M. *Nature*. 2008; 452:580. [PubMed: 18385732]
103. Weissleder R, Ntziachristos V. *Nat. Med*. 2003; 9:123. [PubMed: 12514725]

104. Li N, Ebright J, Stovall G, Chen X, Nguyen H, Singh A, Syrett A, Ellington A. J. *Proteome Res.* 2009; 8:2438. [PubMed: 19271740]
105. Charlton J, Sennello J, Smith D. *Chem. Biol.* 1997; 4:809. [PubMed: 9384527]
106. Chen XL, Estevez MC, Zhu Z, Huang YF, Chen Y, Wang L, Tan WH. *Anal. Chem.* 2009; 81:7009. [PubMed: 19572554]
107. Schäfer R, Wiskirchen J, Guo K, Neumann B, Kehlbach R, Pintaske J, Voth V, Walker T, Scheule A, Greiner TO, Hermanutz-Klein U, Claussen CD, Northoff H, Ziemer G, Wendel HP. *Rofo.* 2007; 179:1009. [PubMed: 17879173]
108. Wang A, Bagalkot V, Vasilliou C, Gu F, Alexis F, Zhang L, Shaikh M, Yuet K, Cima M, Langer R, Kantoff PW, Bander NH, Jon S, Farokhzad OC. *ChemMedChem.* 2008; 3:1311. [PubMed: 18613203]
109. Loai Y, Ganesh T, Cheng H-LM. *Int. J. Mol. Imaging.* 2012; 2012:230942. [PubMed: 22919479]
110. Lopez-Colon D, Jimenez E, You M, Gulbakan B, Tan W. *Wiley Interdiscip. Rev.: Nanomed. Nanobiotechnol.* 2011; 3:328. [PubMed: 21412992]
111. Lendvai G, Estrada S, Bergström M. *Curr. Med. Chem.* 2009; 16:4445. [PubMed: 19835563]
112. Hicke B, Stephens A, Gould T, Chang Y, Lynott C, Heil J, Borkowski S, Hilger C, Cook G, Warren S, Schmidt P. J. *Nucl. Med.* 2006; 47:668. [PubMed: 16595502]
113. Hama Y, Urano Y, Koyama Y, Choyke PL, Kobayashi H. *Cancer Res.* 2007; 67:3809. [PubMed: 17440095]
114. Weissleder R, Tung C-H, Mahmood U, Bogdanov A Jr. *Nat. Biotechnol.* 1999; 17:375. [PubMed: 10207887]
115. Jiang T, Olson E, Nguyen Q, Roy M, Jennings PA, Tsien RY. *Proc. Natl. Acad. Sci. U.S.A.* 2004; 101:17867. [PubMed: 15601762]
116. Blum G, von Degenfeld G, Merchant MJ, Blau HM, Bogoy M. *Nat. Chem. Biol.* 2007; 3:668. [PubMed: 17828252]
117. Kamiya M, Kobayashi H, Hama Y, Koyama Y, Bernardo M, Nagano T, Choyke PL, Urano Y. J. *Am. Chem. Soc.* 2007; 129:3918. [PubMed: 17352471]
118. Olson ES, Jiang T, Aguilera TA, Nguyend QT, Elliese LG, Scadeng M, Tsien RY. *Proc. Natl. Acad. Sci. U.S.A.* 2010; 107:4311. [PubMed: 20160077]
119. Hama Y, Urano Y, Koyama Y, Kamiya M, Bernardo M, Paik RS, Shin IS, Paik CH, Choyke PL, Kobayashi H. *Cancer Res.* 2007; 67:2791. [PubMed: 17363601]
120. Ogawa M, Kosaka N, Longmire MR, Urano Y, Choyke PL, Kobayashi H. *Mol. Pharmaceutics.* 2009; 6:386.
121. Ogawa M, Kosaka N, Choyke PL, Kobayashi H. *Chem. Biol.* 2009; 4:535–546.
122. Shi H, He X, Wang K, Wu X, Ye X, Guo Q, Tan W, Qing Z, Yang X, Zhou B. *Proc. Natl. Acad. Sci. U.S.A.* 2011; 108:3900. [PubMed: 21368158]
123. Urano Y, Asanuma D, Hama Y, Koyama Y, Barrett T, Kamiya M, Nagano T, Watanabe T, Hasegawa A, Choyke PL, Kobayashi H. *Nat. Med.* 2009; 15:104. [PubMed: 19029979]
124. Schmidt KS, Borkowski S, Kurreck J, Stephens AW, Bald R, Hecht M, Friebe M, Dinkelborg L, Erdmann VA. *Nucleic Acids Res.* 2004; 32:5757. [PubMed: 15509871]
125. Wu Y, Sefaha K, Liu H, Wang R, Tan W. *Proc. Natl. Acad. Sci. U.S.A.* 2010; 107:5. [PubMed: 20080797]
126. Lakowicz, J. *Principles of Fluorescence Spectroscopy.* Springer; New York: 1999.
127. Watson SR, Chang YF, O'Connell D, Weigand L, Ringquist S, Parma DH. *Antisense Nucleic Acid Drug Dev.* 2000; 10:63. [PubMed: 10805157]
128. Healy JM, Lewis SD, Kurz M, Boomer RM, Thompson KM, Wilson C, McCauley TG. *Pharm. Res.* 2004; 21:2234. [PubMed: 15648255]
129. Rusconi CP, Roberts JD, Pitoc GA, Nimjee SM, White RR, Quick G Jr, Scardino E, Fay WP, Sullenger BA. *Nat. Biotechnol.* 2004; 22:1423. [PubMed: 15502817]
130. Wu YR, Phillips JA, Liu HP, Yang RH, Tan WH. *ACS Nano.* 2008; 2:2023. [PubMed: 19206447]
131. Fisher KA, Huddersman KD, Taylor MJ. *Chem.-Eur. J.* 2003; 9:5873. [PubMed: 14673859]
132. Lopez T, Quintana P, Martinez JM, Esquivel DJ. *Non-Cryst. Solids.* 2007; 353:987.

133. Tebbe D, Thull R, Gburek U. *Acta Biomater.* 2007; 3:829. [PubMed: 17586106]
134. Wang L, Yang CJ, Medley CD, Benner SA, Tan WJ. *Am. Chem. Soc.* 2005; 127:15664.
135. Yang CJ, Wang L, Wu Y, Kim Y, Medley CD, Lin H, Tan W. *Nucleic Acids Res.* 2007; 35:4030. [PubMed: 17557813]
136. Martinez K, Estevez MC, Wu YR, Phillips JA, Medley CD, Tan WH. *Anal. Chem.* 2009; 81:3448. [PubMed: 19351140]
137. Green LS, Jellinek D, Bell C, Beebe LA, Feistner BD, Gill SC, Jucker FM, Janjic N. *Chem. Biol.* 1995; 2:683. [PubMed: 9383475]

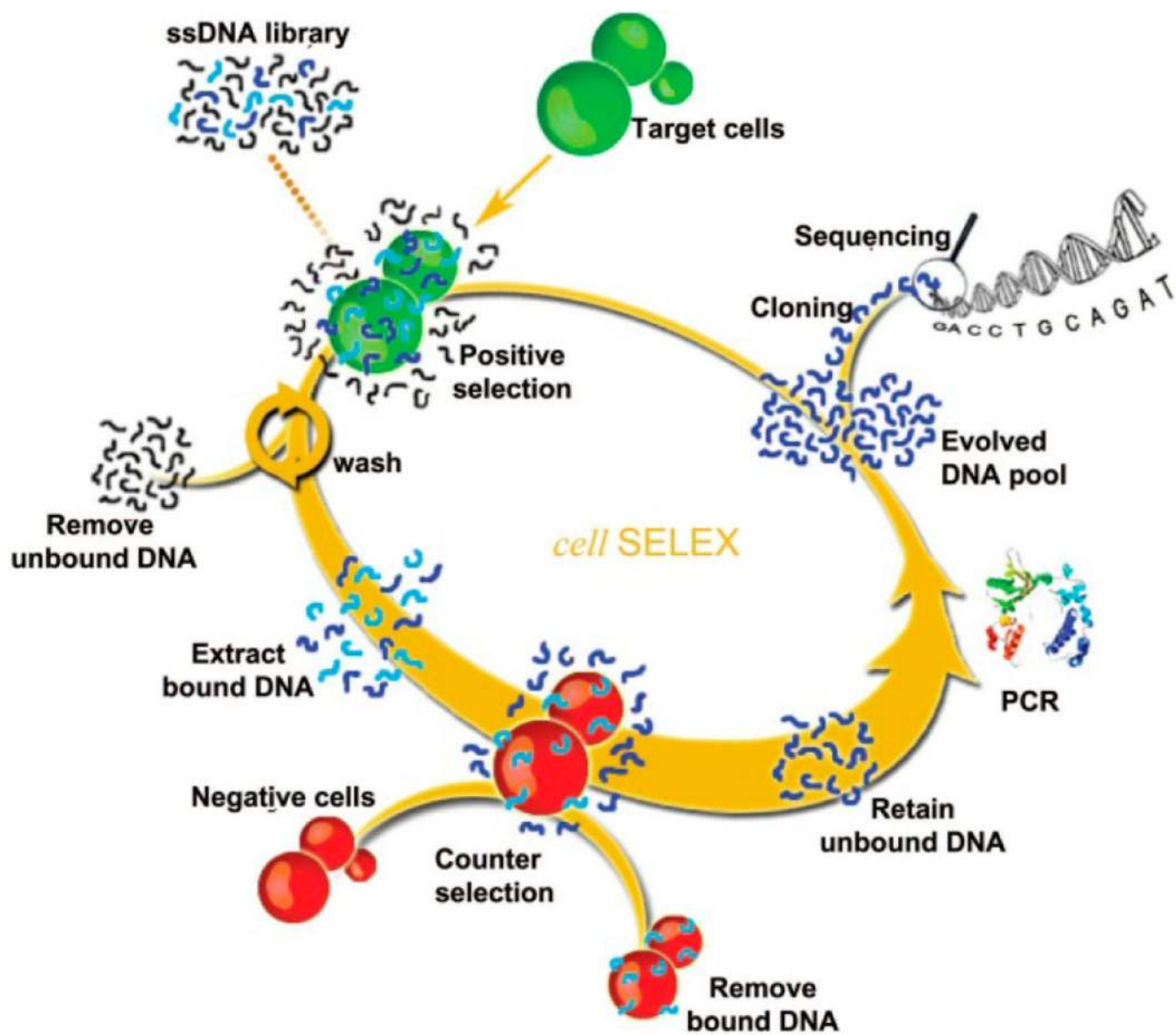


Figure 1. Schematic of cell-SELEX. The process begins with adding ssDNA library in the presence of target cells for incubation and proceeds in a counterclockwise fashion.

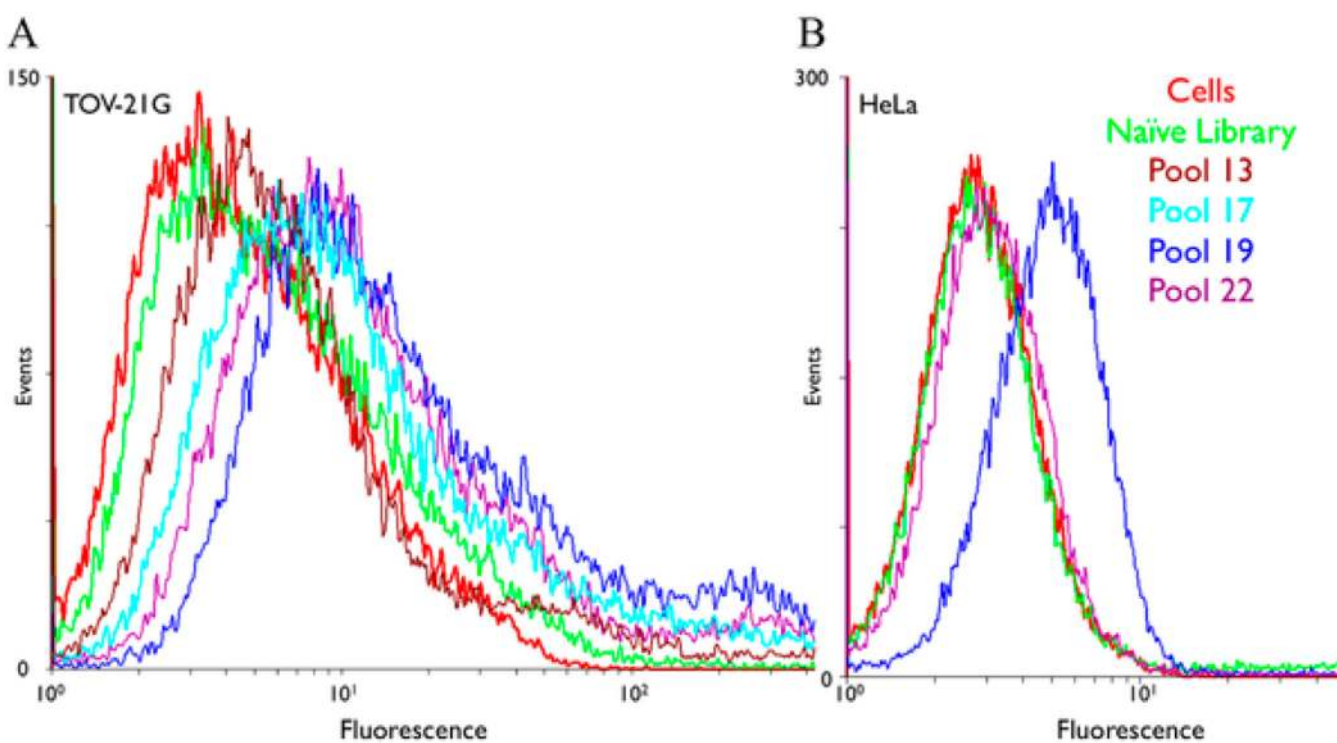


Figure 2. The binding assay of the enriched pools with TOV-21G and HeLa cells. (A) Enrichment with TOV-21G cells and (B) marginal binding of the respective pools to HeLa cells. By doing counter selection, sequences binding to HeLa were removed. Reprinted with permission from ref 27. Copyright 2010 Public Library of Science.

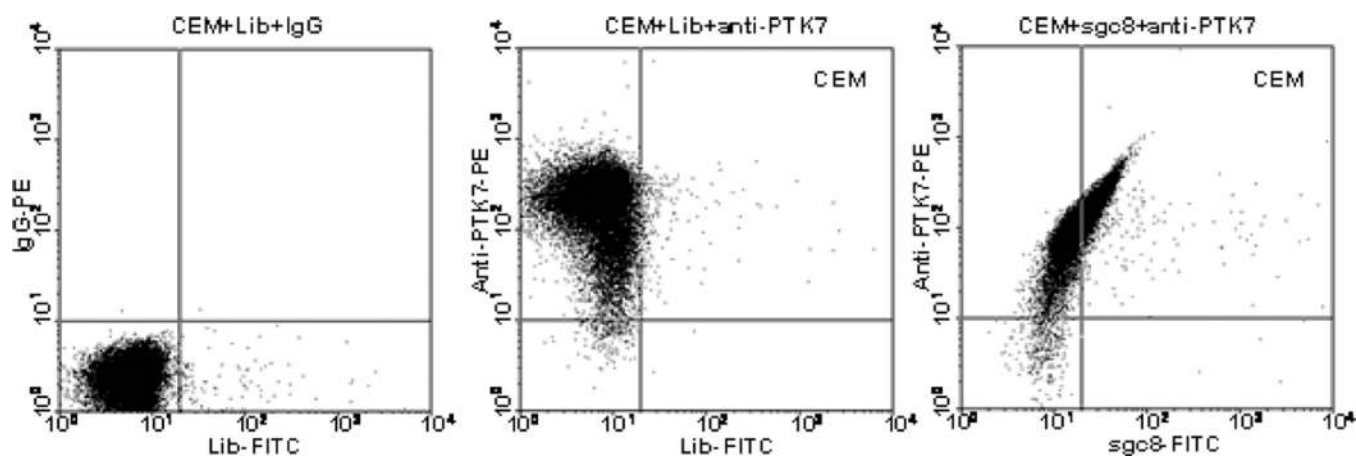


Figure 3.

Flow cytometry analysis of CEM cells targeted with anti-PTK7-PE or sgc8-FITC. Reprinted with permission from Fang, X.; Tan, W. *Acc. Chem. Res.* **2009**, *44*, 48. Copyright 2009 American Chemical Society.

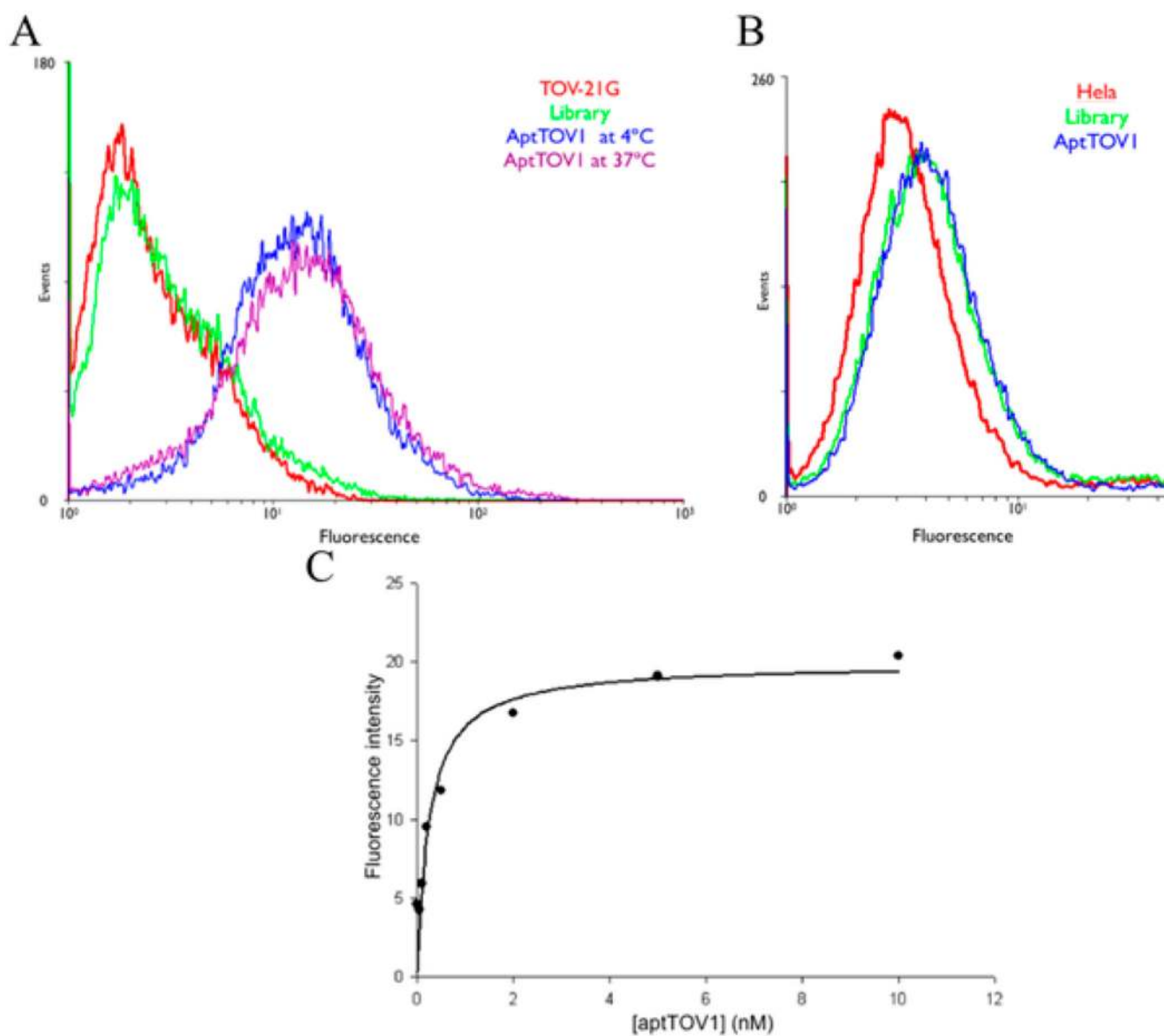


Figure 4.

The binding of PE/Cy5-labeled aptTOV1 (250 nM in binding buffer) (A) to TOV-21G at 4 and 37 °C; and (B) to HeLa at 4 °C. The negative control in these binding assays was PE/Cy5-labeled random library. (C) Cells were incubated with varying concentrations of PE-Cy5-labeled aptamer in duplicate. The fluorescence intensity originating from background binding at each concentration was subtracted from the mean fluorescence intensity of the corresponding aptamer. Reprinted with permission from ref 56. Copyright 2010 Public Library of Science.

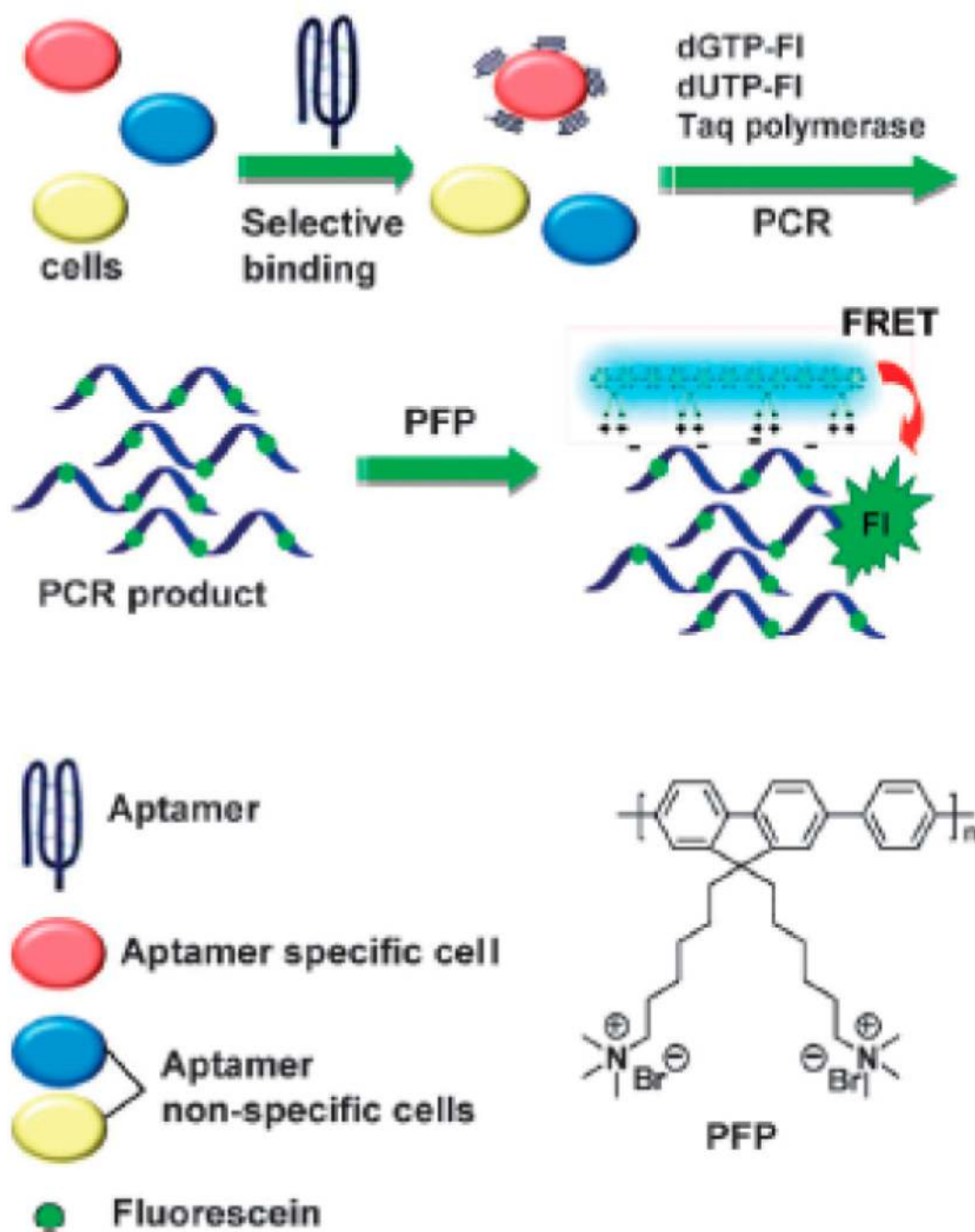


Figure 5. Schematic illustration of aptamer-based PCR strategy for target cell detection. Reprinted with permission from ref 61. Copyright 2012 Royal Society of Chemistry Publishing.

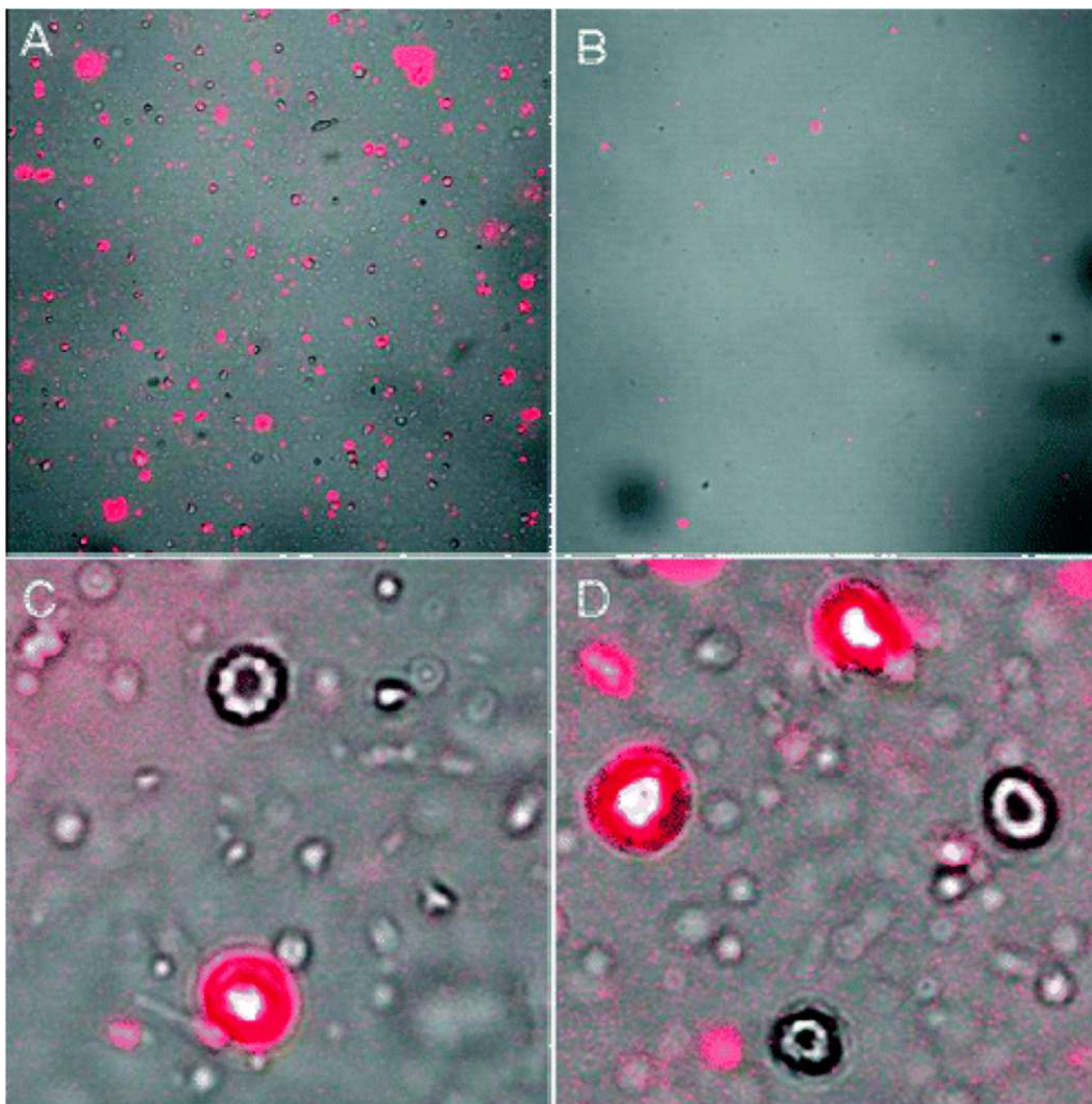


Figure 6. Confocal images of extractions from whole blood. (A) Extracted sample from target cell spiked whole blood. (B) Extraction from unspiked whole blood. (C) and (D) show magnified images of extracted cells with a 1:1 ratio of target cells mixed with Fluo-4-stained control cells. Reprinted with permission from Herr, J.; Smith, J.; Medley, C.; Shangguan, D.; Tan, W. *Anal. Chem.* **2006**, *78*, 2918. Copyright 2006 American Chemical Society.

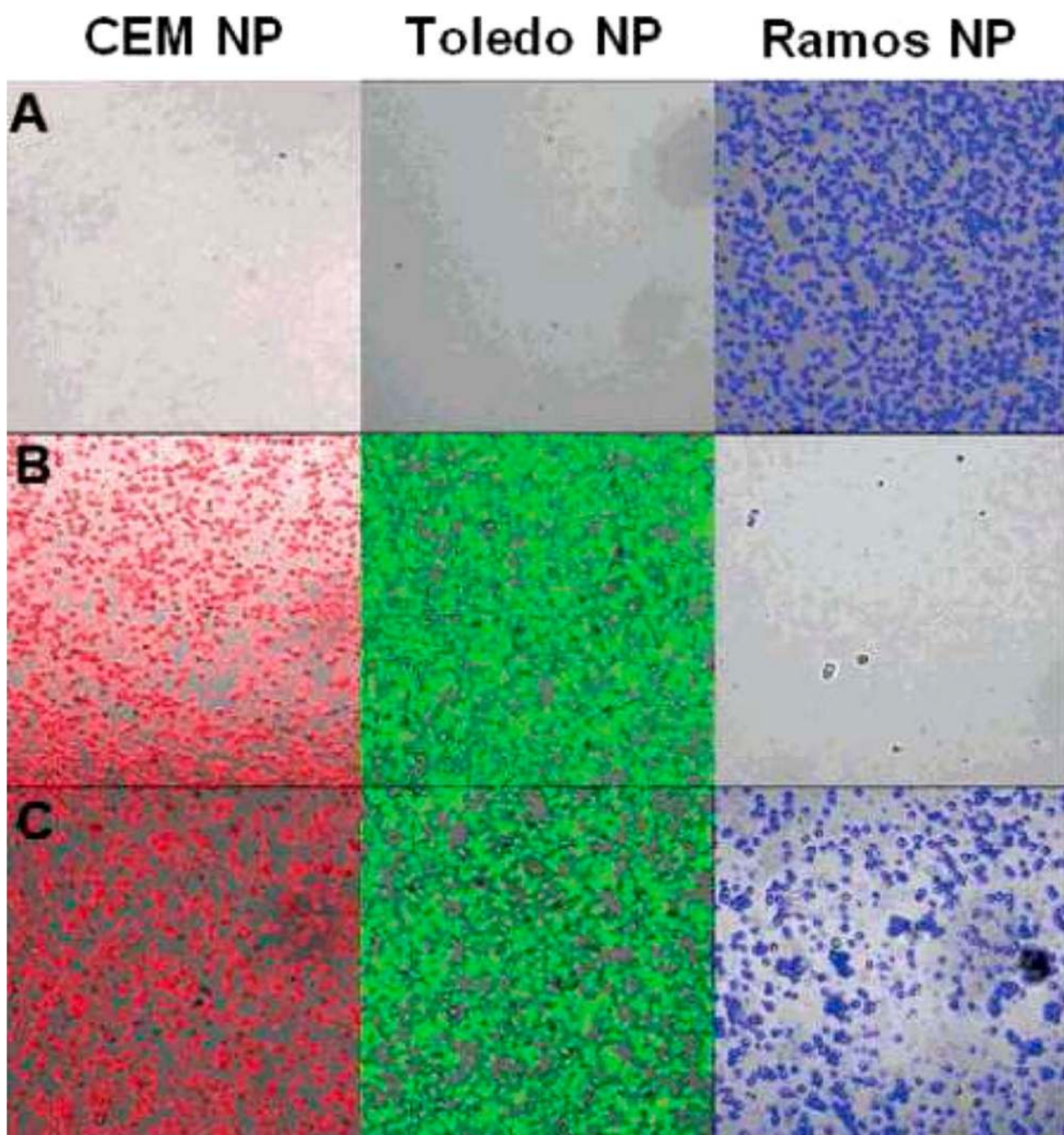


Figure 7.

Fluorescence images of the extracted mixed cell samples using the multiple extraction procedure: (A) contains only Ramos cells; (B) contains CEM and Toledo cells; (C) contains all three, CEM, Toledo, and Ramos cells. Reprinted with permission from Herr, J.; Smith, J.; Medley, C.; Shangguan, D.; Tan, W. *Anal. Chem.* **2006**, *78*, 2918. Copyright 2006 American Chemical Society.

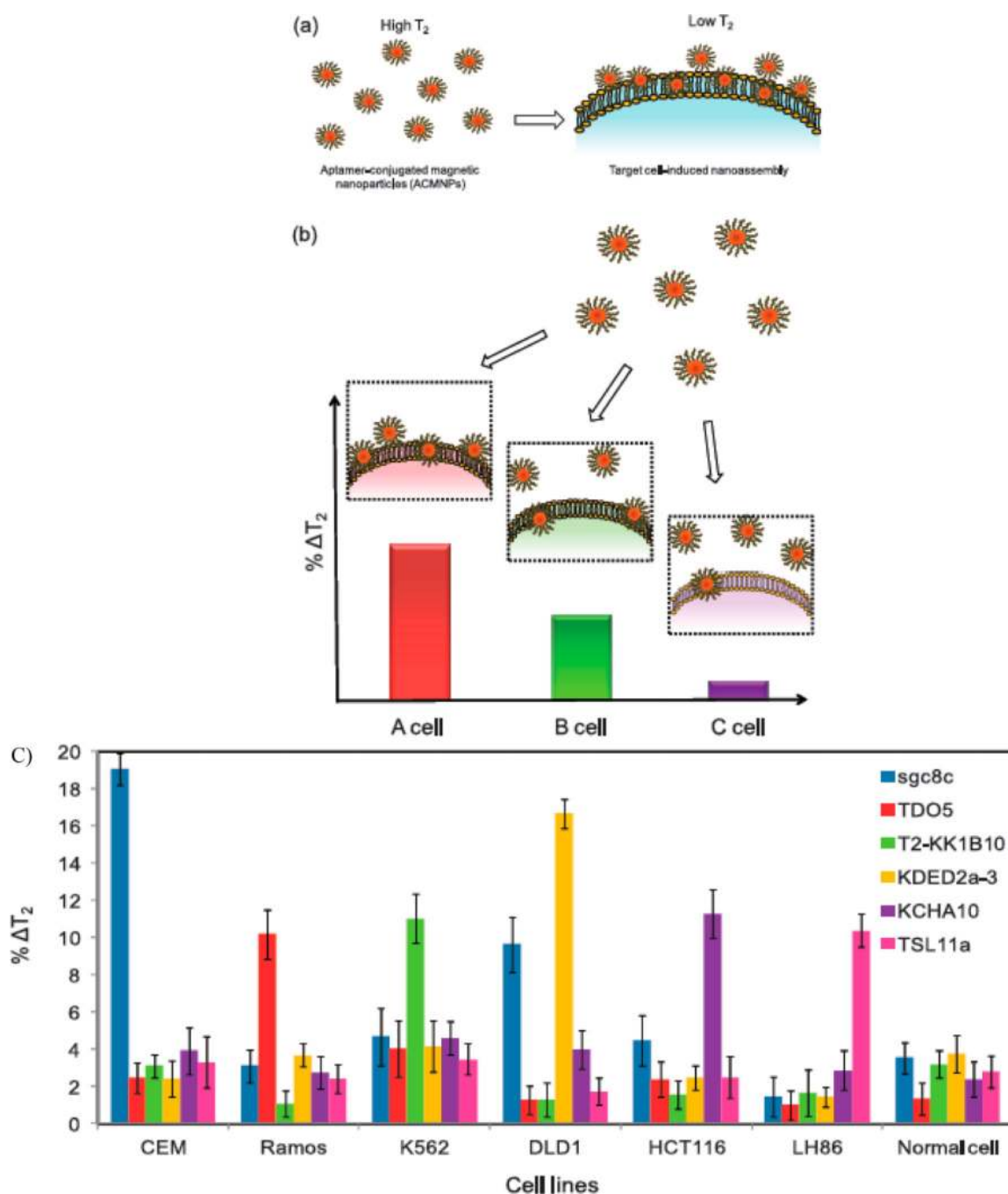


Figure 8. Schematic illustrating the use of a magnetic nanosensor for cancer cell detection and pattern recognition. (a) The magnetic nanoparticles conjugated with aptamers have highly specific binding to their target cells. Without target cells, ACMNPs are well dispersed, resulting in a high T_2 of surrounding water protons. However, the addition of target cells leads to the aggregation of magnetic nanoparticles, decreasing the T_2 of adjacent water protons. (b) Distinct recognition pattern generated for various cell lines with different receptor expression level using the magnetic nanosensor. The cell line with the most abundant (A

cell) receptors gives the largest ΔT_2 , followed by the cell line with an intermediate number of receptors (B cell), and the smallest ΔT_2 was obtained for the cell line with the lowest receptor expression level (C cell). (C) Use of magnetic nanosensors for pattern recognition of cancer cells. The % ΔT_2 was obtained by incubating different ACMNPs with various target cancer cell lines or control normal cell lines. All of the measurements were performed using 1000 cells in a 250 μL sample volume. Reprinted with permission from Bamrungsap, S.; Chen, T.; Shukoor, M.I.; Chen, Z.; Sefah, K.; Chen, Y.; Tan, W. *ACS Nano*. **2012**, *6*, 3974. Copyright 2012 American Chemical Society.

Author Manuscript

Author Manuscript

Author Manuscript

Author Manuscript

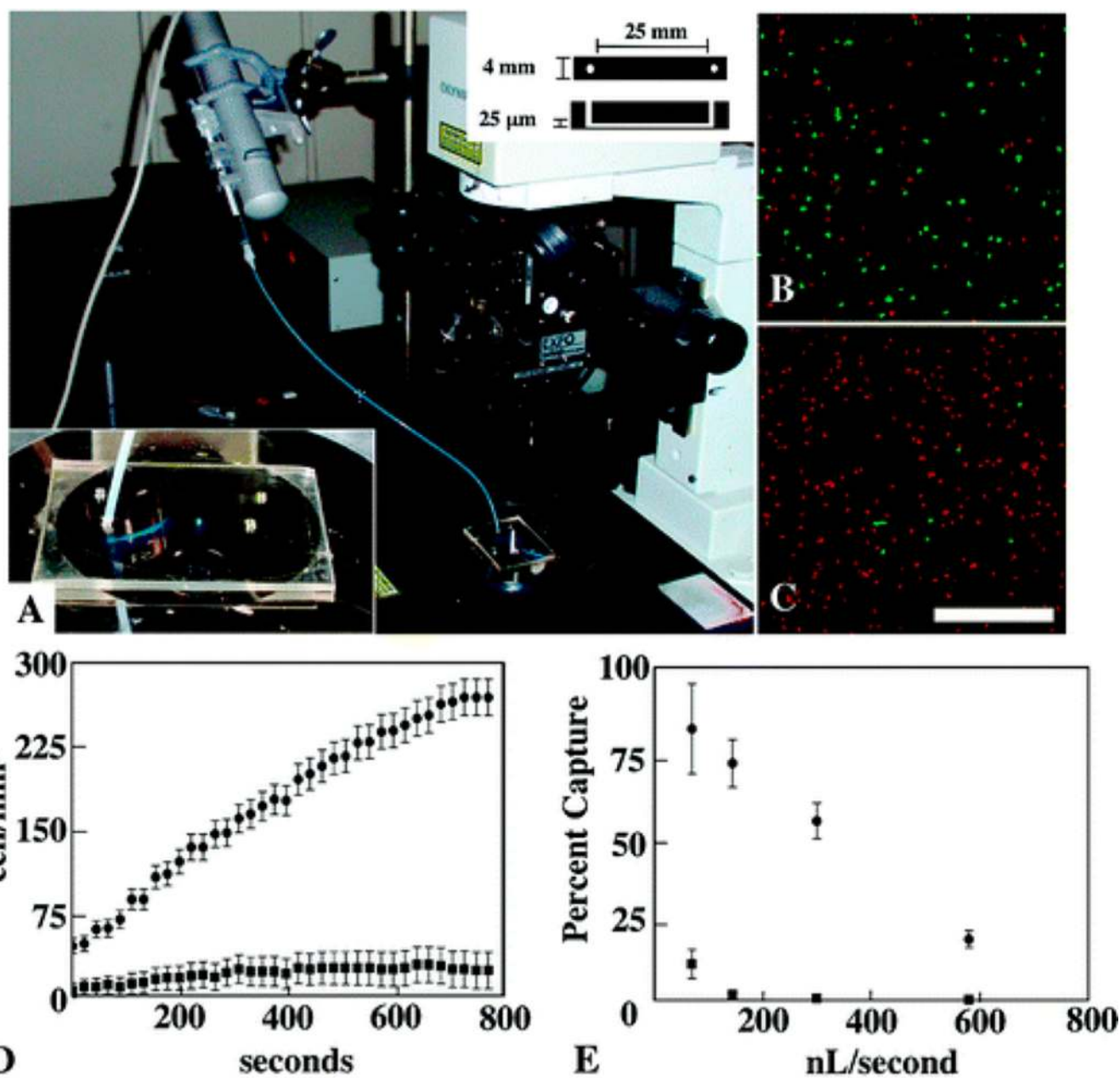


Figure 9. PDMS device with increased cell capture efficiency. Image of device attached to the syringe pump on the confocal microscope (A). The bottom left inlay shows the device, and the top right inlay shows the top-down and sideways views with dimensions. Representative images of the original mixture of cells before the cell capture assay (B) and the channel surface after the cell capture assay was performed at a 154 nL/s flow rate (C), with target and control cells stained red and green, respectively. The cell-surface density measured over the course of the cell capture experiment showing a linear increase in target cells captured over time (D). The target cell capture efficiency decreases with increased fluid flow rate (E). Bar = 500

μm . Reprinted with permission from Phillips, J.; Xu, Y.; Xia, Z.; Fan, Z.; Tan, W. *Anal. Chem.* **2009**, *81*, 1033. Copyright 2009 American Chemical Society.

Author Manuscript

Author Manuscript

Author Manuscript

Author Manuscript

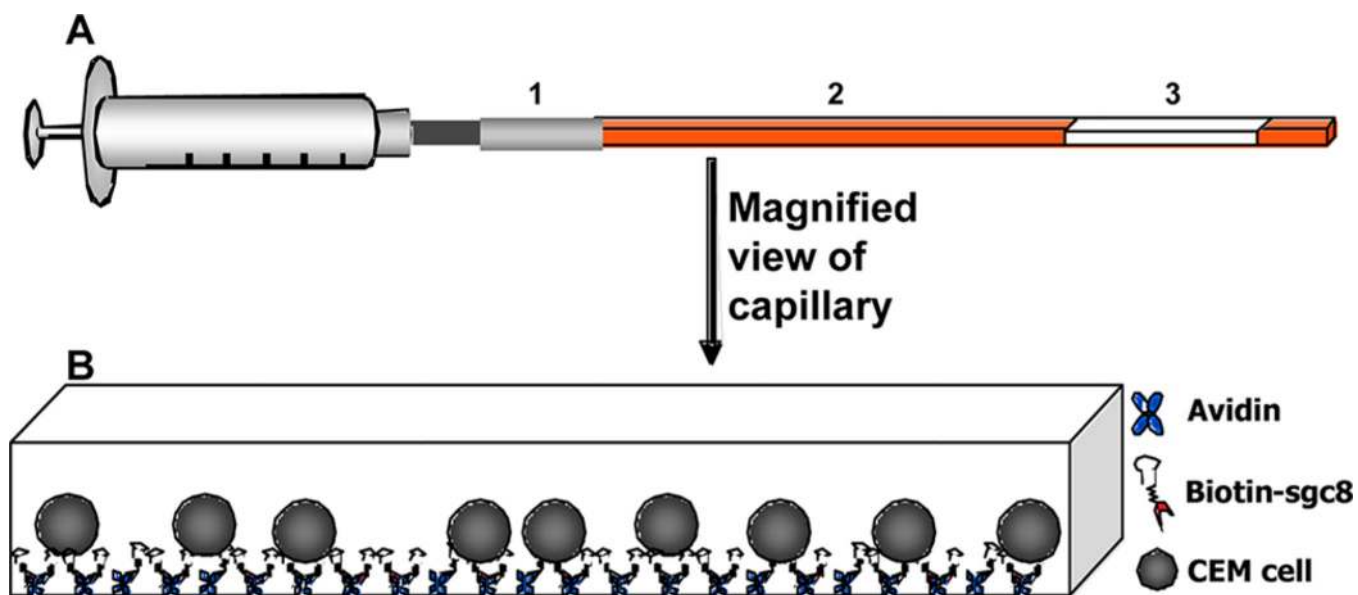


Figure 10. Schematic of square capillary system and immobilization. (A) Syringe with small Teflon tubing connects to square capillary; (B) square capillary is immobilized with avidin, and 5'-FAM-sgc8-poly(T)10-biotin is added for cell capture of CEM cells. Reprinted with permission from ref 87. Copyright 2011 Royal Society of Chemistry Publishing.

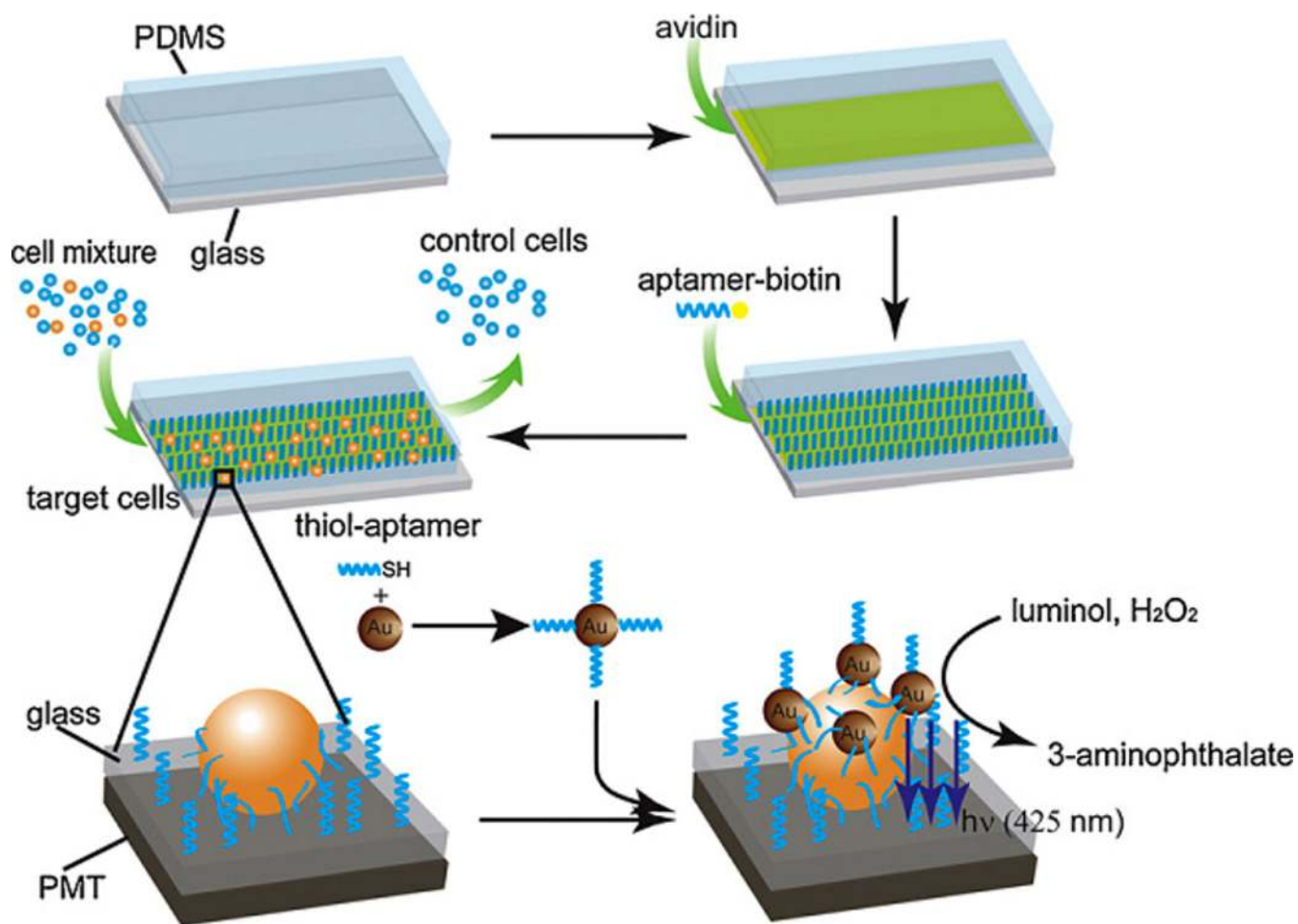


Figure 11. Schematic illustration of chemiluminescence detection platform that incorporates gold colloids with nanoparticles of different sizes. The aptamer-conjugated gold nanoparticles (AC-AuNPs) measure rare cells. Reprinted with permission from Zhang, Z. F.; Cui, H.; Lai, C. Z.; Liu, L. J. *Anal. Chem.* **2005**, *77*, 3324. Copyright 2005 American Chemical Society.

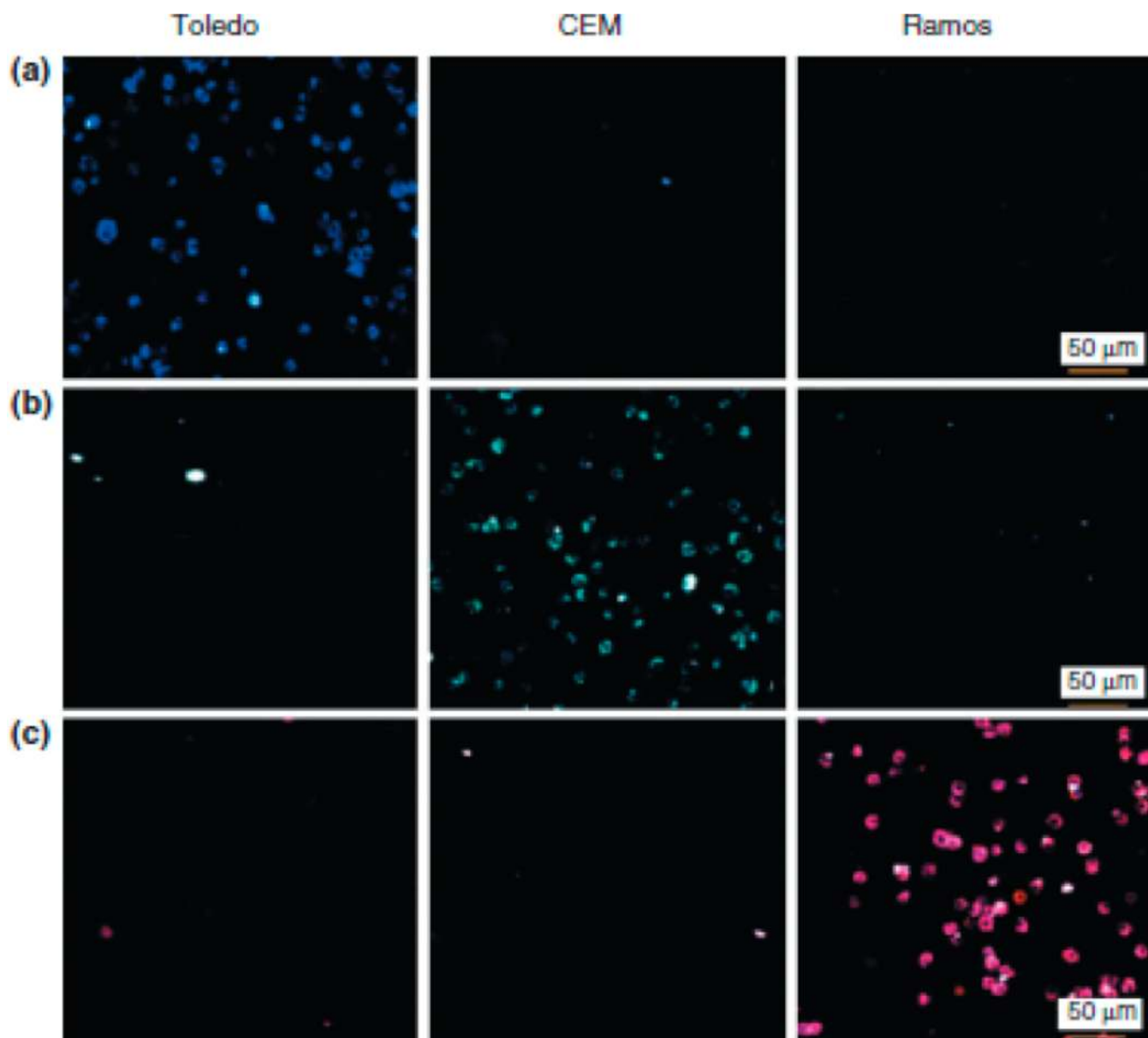


Figure 12.

Confocal microscopy images of individual NP-aptamer conjugates with three different cells (Toledo, CEM, and Ramos): (a) NP (FAM)-T1, (b) NP (FAM-R6G)-sgc8, and (c) NP (FAM-R6G-ROX)-TDO5. Reprinted with permission from Chen, X. L.; Estevez, M. C.; Zhu, Z.; Huang, Y. F.; Chen, Y.; Wang, L.; Tan, W. H. *Anal. Chem.* **2009**, *81*, 7009. Copyright 2009 American Chemical Society.

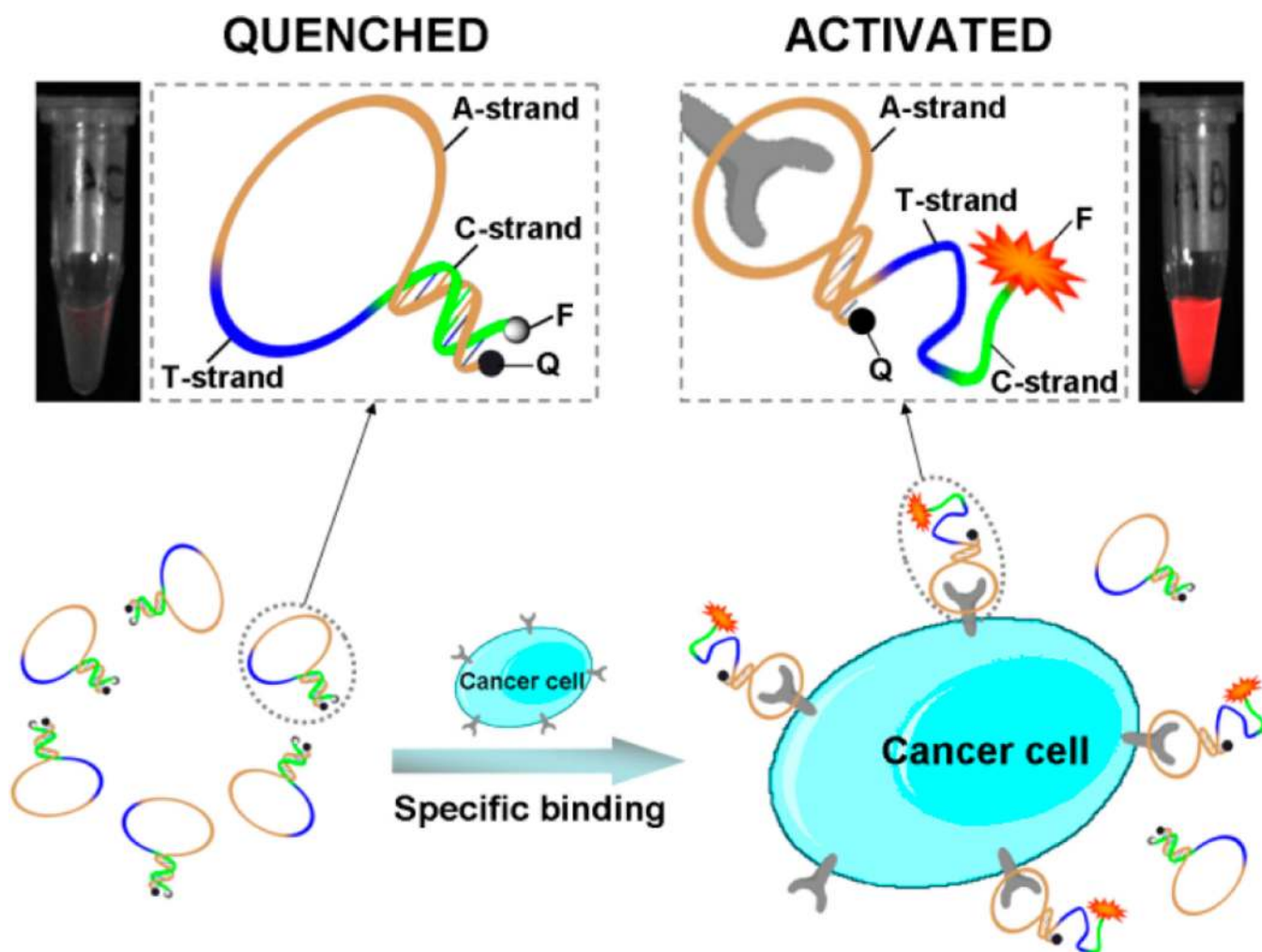


Figure 13. Schematic representation of the novel activatable strategy for in vivo cancer imaging using an activatable aptamer probe (AAP) based on cell membrane protein-triggered conformation alteration. The AAP consists of three components: a cancer-targeted aptamer sequence (A-strand), a poly-T linker (T-strand), and a short DNA sequence (C-strand) complementary to a part of the A-strand, with a fluorophore and a quencher attached at either terminus. In the absence of a target, the AAP is hairpin structured, resulting in quenched fluorescence. When the probe is bound to membrane receptors of the target cancer cell, its conformation is altered, thus leading to an activated fluorescence signal. Reprinted with permission from ref 122. Copyright 2011 United States National Academy of Sciences.

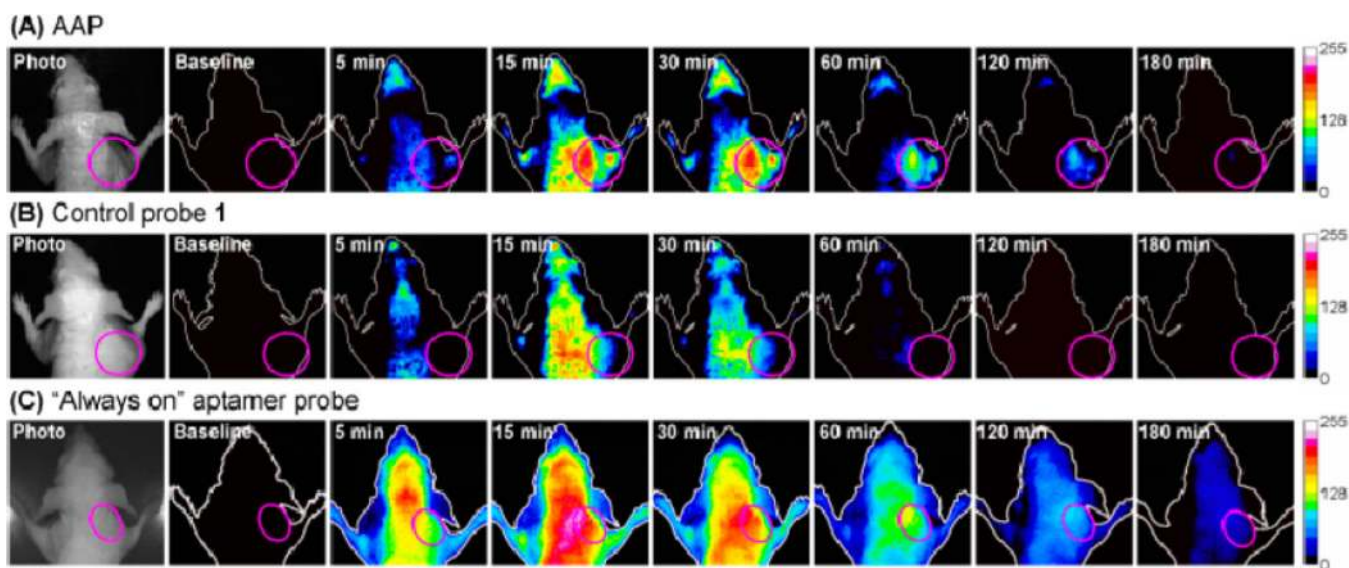


Figure 14.

In vivo time-dependent fluorescence imaging of CCRF-CEM tumors. CCRF-CEM tumor-bearing nude mice were intravenously injected with (A) the AAP, (B) control probe 1, and (C) the “always on” aptamer probe, respectively. Fluorescence images of the dorsal side of live mice were then taken at several specified postinjection time points. Time of exposure for every fluorescence image was 1000 ms in groups (A) and (B) and 100 ms in group (C). The pink circle in every image locates the tumor site. . Reprinted with permission from ref 122. Copyright 2011 United States National Academy of Sciences.

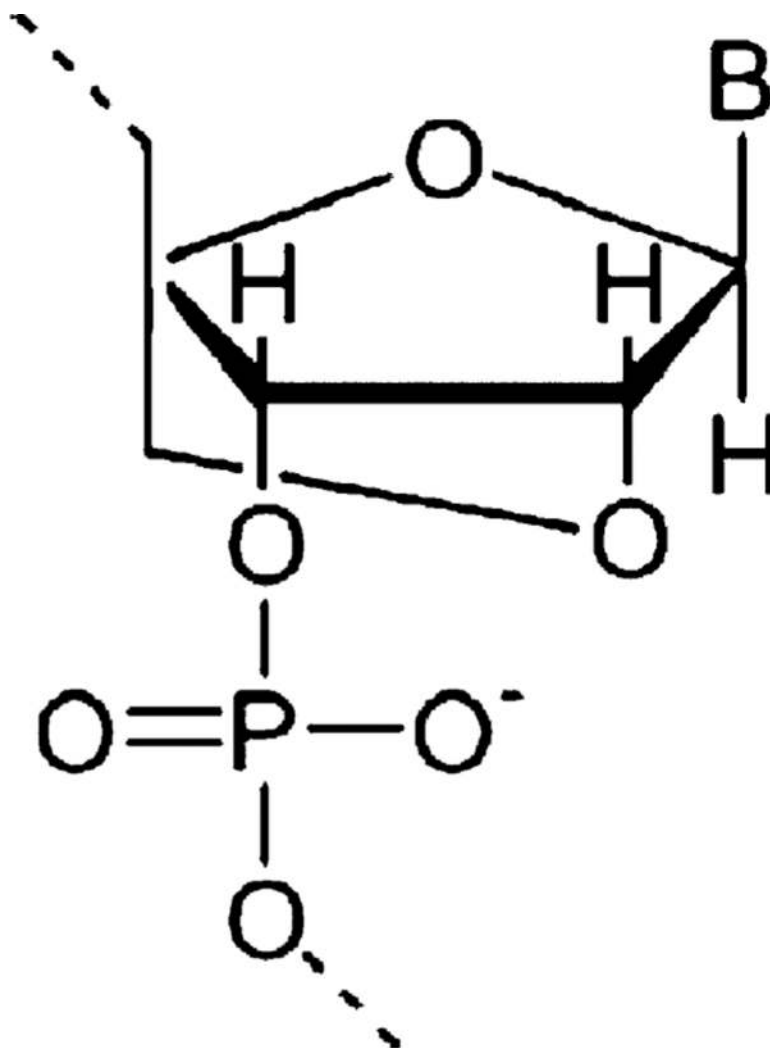


Figure 15.
Structure of locked nucleic acid (LNA).

Table 1

Examples of Positive and Negative Cell Lines That Have Been Successfully Paired To Generate High-Affinity and Specific Aptamers^a

positive	description	negative	description
CCRF-CEM	T-cell line, human ALL	Ramos	B-cell line, human Burkitt's lymphoma ²¹
NCI-H69	carcinoma; small-cell lung cancer	NCI-H661	carcinoma; large-cell lung cancer ²²
BNL 1ME A.7R.1 (MEAR)	mouse liver hepatoma cell line	BNL CL.2	normal mouse liver cell line ¹⁴
HL60	acute myeloid leukemia	NB4	acute promyelocytic leukemia ¹²
A549	human lung carcinoma cells infected with vaccinia virus	A549	human lung carcinoma cells without infection ²⁶

^aReprinted with permission from ref 25. Copyright 2010 Nature Publishing Group.

Abbreviation: ALL, acute lymphoblastic leukemia.

Table 2

Summary of Aptamers Generated by Cell-SELEX

	target type	target cell line	no. of aptamers	best K_d (nM)	patient testing
leukemia	T-ALL	CEM	10	0.8 ± 0.09	bone marrow
	B-ALL	Ramos	13	0.76 ± 0.13	bone marrow
	AML	HL-60	8	4.5 ± 1.6	bone marrow
liver cancer		MEAR	8	4.51 ± 0.39	mice tumor
lung cancer	SCLC	NCI-H69	4	~38	blood samples
	NSCLC	A549	9	28.2 ± 5.5	tissue section
ovarian cancer	ovarian clear cell adenocarcinoma	TOV-21G	10	0.25 ± 0.08	N.D.
	ovarian serous adenocarcinoma	CAOV-3	3	39 ± 20	N.D.
colorectal cancer		DLD-1	7	32.1 ± 3.4	N.D.
		HCT 116	9	3.9 ± 0.4	N.D.
brain tumor	glioblastoma multiforme	A172	5	61.82 ± 6.37	N.D.
virus-infected cells:	vaccinia virus-infected	A549	12	1.45 ± 0.3	N.D.
mature adipocytes		3T3-L1	10	30 ± 3.6	N.D.

Table 3SELEX Library Affinities (K_d , M) with Unmodified and Modified Nucleotides^a

target protein	dT	BndU	iBudU	TrpdU
4-1BB ^b	failed	6×10^{-9}	failed	4×10^{-9}
B7 ^b	failed	1×10^{-8}	failed	7×10^{-9}
B7-2 ^b	failed	failed	failed	6×10^{-9}
CTLA-4 ^b	failed	failed	failed	1×10^{-9}
sE-selectin ^b	failed	failed	failed	2×10^{-9}
fractalkine/CX3CL-1	failed	failed	failed	5×10^{-11}
GA733-1 protein ^b	9×10^{-9}	3×10^{-9}	5×10^{-9}	5×10^{-10}
gp130, soluble ^b	failed	6×10^{-9}	2×10^{-8}	1×10^{-9}
HMG-1	failed	failed	2×10^{-8}	5×10^{-9}
IR	failed	2×10^{-9}	1×10^{-8}	2×10^{-10}
osteoprotegerin ^b	4×10^{-8}	5×10^{-9}	9×10^{-9}	2×10^{-10}
PAI-1	failed	4×10^{-10}	9×10^{-10}	2×10^{-10}
P-cadherin ^b	failed	4×10^{-9}	5×10^{-9}	3×10^{-9}
sLeptin R ^b	failed	2×10^{-9}	failed	5×10^{-10}

^aReprinted with permission from ref 35. Copyright 2010 Public Library of Science.^bThe protein used was expressed as a fusion to the Fc of human IgG1. No detectable binding of the active library to an alternate Fc fusion protein was observed.

Table 4

A Compendium of the Aptamers Obtained by Selection for Cancer Cell Lines TOV-21G (aptTOV) or CAOv-3 (DOV)^a

name	Sequence	K_a (nM)	% in pool
aptTov1	5'-ATC CAG AGT GAC GCA GCA GAT CTG TGT AGG ATC GCA GTG TAG TGG ACA TTT GAT ACG ACT GGt TCG ACA CM TGG CTT A-3'	0.25 ± 0.08	2.53
aptTov2	5'-ATC CAG AGT GAC GCA GCA TAA TCT CTA CAG GCG CAT GTA ATA TAA TGA AGC CCA TCC ACC TGG ACA CGG TGG CTT A-3'	0.90 ± 0.25	18.62
aptTov2a	5'-ATC CAG AGT GAC GCA GCA CAA TCT CTA CAG GCG CAT GTA ATA TAA TGG AGC CTA TCC ACG TCG ACA CGG TGG CTT A-3'	11 ± 3	7.65
aptTov3	5' -ATC CAG AGT GAC GCA GCA CTC ACT CTG ACC TTG GAT CGT CAC ATT ACA TGG GAT CAT CAG TCG ACA CGG TGG CTT A-3'	30 ± 9	8.74
aptTov4	5'-ATC CAG AGT GAC GCA GCA GGC ACT CTT CAC AAC ACG ACA TTT CAC TAC TCA CAA TCA CTC TCG ACA CGG TGG CTT A-3'	20 ± 5	0.52
aptTov5	5'-ATC CAG AGT GAC GCA GCA CAA CAT CCA CTC ATA ACT TCA ATA CAT ATC TGT CAC TCT TTC TCG ACA CGG TGG CTT A-3'	4.5 ± 1.2	0.82
aptTov6	5'-ATC CAG AGT GAC GCA GCA CGG CAC TCA CTC TTT GTT AAG TGG TCT GCT TCT TAA CCT TCA TCG ACA CGG TGG CTT A-3'	29 ± 7	0.58
aptTov7	5'-ATC CAG AGT GAC GCA GCA CCA ACT CGT ACA TCC TTC ACT TAA TCC GTC AAT CTA CCA CTC TCG ACA CGG TGG CTT A-3'	6.6 ± 2.3	0.19
aptTov8	5'-ATC CAG AGT GAC GCA GCA CCA GTC CAT CCC AAA ATC TGT CGT CAC ATA CCC TGC TGC GCC TCG ACA CGG TGG CTT A-3'	17 ± 3	0.76
aptTov9	5'-ATC CAG AGT GAC GCA GCA GCA ACA CAA ACC CAA CTT CTT ATC TTT TCG TTC ACT CTT CTC TCG ACA CGG TGG CTT A-3'	26 ± 10	0.06
DOV3	5'-ACT CAA CGA ACG CTG TGG ATG CAG AGG CTA GGATCT ATA GGT TCGGAC GTC GAT GAG GAC CAG GAG AGC A-3'	132 ± 32	ND
DOV4	5'-ACT CAA CGA ACG CTG TGG AGG GCA TCA GAT TAG GAT TAG GAT CTA TAG GTTCGG ACA TCG TGA GGA CCA GGA GAG CA-3'	40 ± 20	ND
DOV6	5'-ACT CAA CGA ACG CTG TGG AAT GTT GGGGTA GGT AGA AGG TGA AGGGGT TTC AGT TGA GGA CCA GGA GAG CA-3'	39 ± 20	ND

^aReprinted with permission from ref 56. Copyright 2010 Public Library of Science.

Table 5

Using Aptamers To Recognize Cancer Cells

cell line	Sgc8	Sgc3	Sgc4	Sgd2	Sgd3
cultured cell line	+++	+++	++++	++++	++++
Molt-4 (T cell ALL)	+++	+	++++	++++	++
Sup-T1 (T cell ALL)	++++	+++	++++	++++	++++
Jurkat (T cell ALL)	+	0	++	+	0
SUP-B15 (B cell ALL)	0	0	0	0	0
U266 (B cell myeloma)	0	0	++++	++++	+
Toledo (B cell lymphoma)	0	++	++	0	+
NB-4 (AML, APL) cells from patients	0	0	+++	+++	0
T cell ALL	++	+++	+++	+++	+++
Large B cell lymphoma	0	0	0	0	0